Article

Cell

A Cold-Sensing Receptor Encoded by a Glutamate Receptor Gene

Graphical Abstract

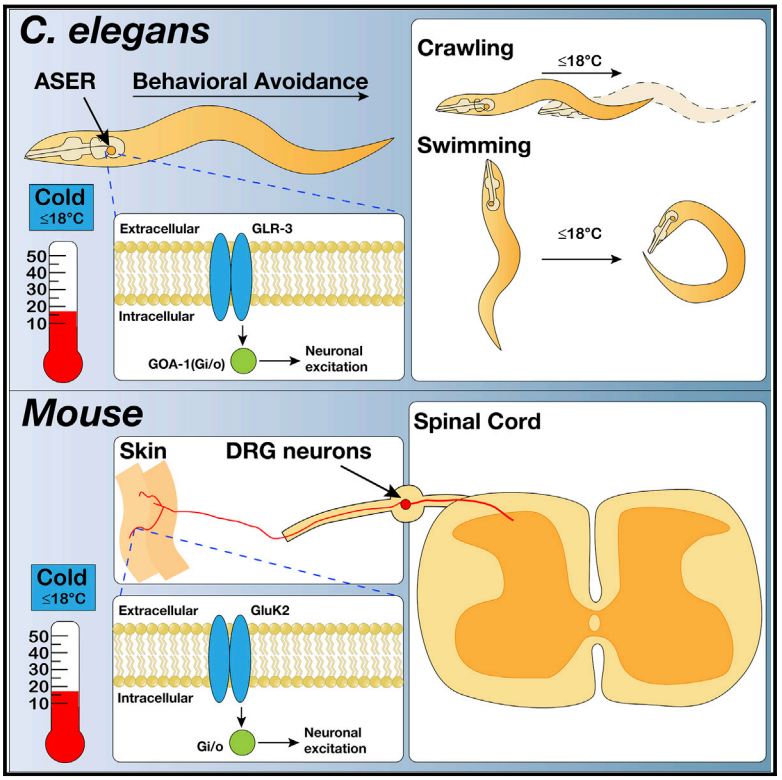

Highlights

- *C. elegans* genetic screen identifies the glutamate receptor GLR-3 as a cold receptor
- GLR-3 senses cold in a peripheral sensory neuron to trigger cold-avoidance behavior
- GLR-3 is a metabotropic cold receptor requiring G proteins to transmit cold signals
- The mouse GLR-3 homolog GluK2 acts in DRG sensory neurons to mediate cold sensation

Authors

Jianke Gong, Jinzhi Liu, Elizabeth A. Ronan, ..., Bo Duan, Jianfeng Liu, X.Z. Shawn Xu

Correspondence

jfliu@mail.hust.edu.cn (J.L.), shawnxu@umich.edu (X.Z.S.X.)

In Brief

An evolutionarily conserved cold sensor, which is encoded by a glutamate receptor gene, transmits cold signals through G-protein signaling, independent of its channel function.

Gong et al., 2019, Cell *178*, 1375–1386
September 5, 2019
https://doi.org/10.1016/j.cell.2019.07.034

CellPress

Cell

A Cold-Sensing Receptor Encoded by a Glutamate Receptor Gene

Jianke Gong,[1,2,3,9] Jinzhi Liu,[1,2,3,9] Elizabeth A. Ronan,[2,3,9] Feiteng He,[1,2,3,9] Wei Cai,[2,3] Mahar Fatima,[4] Wenyuan Zhang,[1,2,3] Hankyu Lee,[4] Zhaoyu Li,[2,3,8] Gun-Ho Kim,[7] Kevin P. Pipe,[5,6] Bo Duan,[4] Jianfeng Liu,[1,*] and X.Z. Shawn Xu[2,3,10,*]

[1]College of Life Science and Technology, Key Laboratory of Molecular Biophysics of MOE, and International Research Center for Sensory Biology and Technology of MOST, Huazhong University of Science and Technology, Wuhan, Hubei 430074, China
[2]Life Sciences Institute, University of Michigan, Ann Arbor, MI 48109, USA
[3]Department of Molecular and Integrative Physiology, University of Michigan, Ann Arbor, MI 48109, USA
[4]Department of Molecular, Cellular, and Developmental Biology, University of Michigan, Ann Arbor, MI 48109, USA
[5]Department of Mechanical Engineering, University of Michigan, Ann Arbor, MI 48109, USA
[6]Department of Electrical Engineering and Computer Science, University of Michigan, Ann Arbor, MI 48109, USA
[7]Department of Mechanical Engineering, Ulsan National Institute of Science and Technology, 50 UNIST-gil, South Korea
[8]Present address: Queensland Brain Institute, University of Queensland, St. Lucia QLD 4072, Australia
[9]These authors contributed equally
[10]Lead Contact
*Correspondence: jfliu@mail.hust.edu.cn (J.L.), shawnxu@umich.edu (X.Z.S.X.)
https://doi.org/10.1016/j.cell.2019.07.034

SUMMARY

In search of the molecular identities of cold-sensing receptors, we carried out an unbiased genetic screen for cold-sensing mutants in *C. elegans* and isolated a mutant allele of *glr-3* gene that encodes a kainate-type glutamate receptor. While glutamate receptors are best known to transmit chemical synaptic signals in the CNS, we show that GLR-3 senses cold in the peripheral sensory neuron ASER to trigger cold-avoidance behavior. GLR-3 transmits cold signals via G protein signaling independently of its glutamate-gated channel function, suggesting GLR-3 as a metabotropic cold receptor. The vertebrate GLR-3 homolog GluK2 from zebrafish, mouse, and human can all function as a cold receptor in heterologous systems. Mouse DRG sensory neurons express GluK2, and GluK2 knockdown in these neurons suppresses their sensitivity to cold but not cool temperatures. Our study identifies an evolutionarily conserved cold receptor, revealing that a central chemical receptor unexpectedly functions as a thermal receptor in the periphery.

INTRODUCTION

The ability to sense cold is essential for life. Cold temperatures trigger profound physiological and behavioral responses in nearly every organism (Bandell et al., 2007; Schepers and Ringkamp, 2010). For example, cold stimuli, particularly noxious cold, are not only life-threatening, but also cause severe tissue damage and evoke pain in animals and humans (Foulkes and Wood, 2007). To survive, organisms have evolved exquisite thermosensory systems to detect and react to cold temperatures (Bandell et al., 2007; Schepers and Ringkamp, 2010). Molecular cold sensors are a central player in cold sensation (Bandell et al., 2007; Schepers and Ringkamp, 2010). These cold receptors, which are expressed in cold-sensitive neurons/cells in the periphery, sense cold temperatures and relay the signals to the central nervous system (CNS) to trigger nocifensive behaviors and elicit pain (Schepers and Ringkamp, 2010).

Despite decades of intensive research, little is known about the molecular mechanisms underlying cold sensation. Thus far, only one cold receptor, TRPM8, which is a TRP family channel, has been verified both *in vivo* and *in vitro* in mammals. TRPM8 senses cool temperatures with an activation threshold at ~26°C and mediates cool sensation in mice (Bautista et al., 2007; Dhaka et al., 2007; McKemy et al., 2002; Peier et al., 2002). Some other mammalian TRP channels (e.g., TRPA1) have also been suggested as a cold receptor, but their function in thermosensation appears complex and remains to be defined (Moparthi et al., 2016; Story et al., 2003; Vandewauw et al., 2018; Winter et al., 2017). As such, the molecular identities of cold receptors remain largely elusive. Because animals and humans are clearly capable of sensing temperatures below 26°C, and TRPM8 knockout mice show robust responses to noxious cold (Bautista et al., 2007; Dhaka et al., 2007), unknown cold receptors, particularly those sensing noxious cold, must exist but remain to be identified.

Glutamate receptors, such as kainate, AMPA, and NMDA receptors, are glutamate-gated ion channels that are primarily expressed in the brain. These chemical-sensing receptors transmit chemical signals between neurons and mediate the majority of excitatory chemical synaptic transmission in the CNS (Traynelis et al., 2010). These receptors also mediate synaptic plasticity in the CNS, which underlies learning and memory (Traynelis et al., 2010). Dysfunction of glutamate receptors leads to a wide variety of CNS disorders, ranging from epilepsy, ischemic stroke, and neurodegeneration (e.g., Alzheimer's disease and Parkinson's disease), to mental retardation (Bowie, 2008).

Together, these highlight a fundamental role of glutamate receptors in the function and organization of the CNS.

Here, we designed an unbiased, activity-based genetic screen for cold receptors in *C. elegans*, a model organism widely used for the study of sensory biology (Bargmann, 2006; Garrity et al., 2010; Goodman, 2006; Ward et al., 2008). To do so, we employed a real-time PCR thermocycler, which allowed us to conduct a high throughput genetic screen for mutants defective in cold sensation using live animals. We identify GLR-3, a kainate-type glutamate receptor homolog, as a cold receptor. GLR-3 senses cold temperatures in the sensory neuron ASER to trigger cold-avoidance behavior, indicating that GLR-3 functions in the peripheral nervous system to mediate cold sensation. Heterologous expression of GLR-3 in mammalian cell lines confers cold sensitivity, suggesting that it is sufficient to function as a cold receptor. The activation threshold of GLR-3 is below 20°C, suggesting that it mainly senses noxious cold rather than cool temperatures. Surprisingly, GLR-3 functions as a metabotropic cold receptor rather than a typical temperature-gated ion channel, and its role in cold sensation is independent of its glutamate receptor function. The GLR-3 homolog GluK2 from fish, mouse, and human can all function as a cold receptor *in vitro*, and mouse GluK2 can functionally substitute for GLR-3 *in vivo*. Mouse GluK2 is expressed in dorsal root ganglion (DRG) sensory neurons, and knockdown of GluK2 in DRG neurons suppresses the sensitivity of these sensory neurons to cold but not cool temperatures. Our studies identify an evolutionarily conserved cold receptor. As glutamate receptors are best known to transmit chemical signals across synapses in the CNS, our studies also present a striking case where a central chemical receptor functions as a thermal receptor in the periphery.

RESULTS

Designing an Unbiased, Activity-Based Genetic Screen for Cold Receptors

Previous efforts to identify cold receptors mostly focused on the use of candidate gene approaches but not unbiased genetic screens (Bandell et al., 2007; Castillo et al., 2018). Those cold receptors that do not fall into the category of known thermosensors (e.g., TRP family channels) would thus have escaped detection. To overcome this difficulty, one approach is to design and conduct an unbiased screen, which has the potential to uncover new types of cold receptors.

Thus, we sought to design a forward genetic screen for mutants defective in cold sensation in *C. elegans*, an organism widely used as a genetic model for sensory biology. Traditionally, behavioral assays are employed to conduct such a genetic screen in *C. elegans*. Despite its convenience, this type of screen lacks specificity, as the phenotype in isolated mutants might simply result from defects in sensory processing by downstream neural circuits rather than in cold sensing by sensory neurons/cells. We thus decided to design an activity-based genetic screen by directly targeting sensory neurons/cells.

We previously reported that worm intestinal cells directly sense cold (Xiao et al., 2013). Cooling induces robust calcium response in the intestine dissected out of the worm, shown by calcium imaging using the genetically encoded calcium sensor GCaMP (Xiao et al., 2013). The intestine is the largest worm tissue composed of 20 epithelial cells (McGhee, 2007). The large size of the intestine makes it possible to conduct a high throughput activity-based screen by monitoring cooling-triggered calcium response in the intestine. To design such a screen, we considered using a real-time PCR thermal cycler that is designed for amplifying and quantifying cDNA (Figure 1A). This type of equipment can rapidly and precisely cool/heat the sample while monitoring changes in the fluorescence (e.g., GCaMP) level of the sample in real time. This feature and the convenience that worms can readily fit into PCR tubes motivated us to employ such a thermal cycler to conduct a high throughput activity-based screen using live worms (Figure 1A). Though TRPA-1 contributes to cold-evoked calcium response in the intestine, robust cold response persists in *trpa-1* mutant worms (Xiao et al., 2013), indicating the presence of unknown cold receptor(s). We thus performed a large scale chemical mutagenesis screen for such unknown cold receptor(s) using this strategy (Figure 1A).

glr-3 Mutants Show a Strong Defect in Cooling-Evoked Calcium Response

After screening >30,000 F2 strains, we recovered 11 mutants. We focused on *xu261*, a mutant allele that showed a strong phenotype in cooling-evoked calcium response (Figure 1A). By whole-genome sequencing, we mapped the mutation to the *glr-3* gene that encodes a kainate-type glutamate receptor (Brockie et al., 2001; Figure 1A).

To further characterize GLR-3, we performed standard calcium imaging experiments by fluorescence microscopy. We found that *glr-3* null mutant worms (i.e., *glr-3*(*tm6403*)) displayed a severe defect in cooling-evoked calcium increase in the intestine, a phenotype that was rescued by transgenic expression of wild type *glr-3* gene in the intestine using an intestine-specific promoter (Figures 1B and 1C). *glr-3*(*xu261*) mutant worms also displayed a similar phenotype (Figure S1). These results identify a key role for GLR-3 in mediating cooling-evoked cold response in the intestine.

The Sensory Neuron ASER Is Cold-Sensitive and Requires GLR-3 to Sense Cold

We next set out to characterize the *in vivo* functions of GLR-3 in cold sensation. GLR-3 has been reported to be expressed in central neurons (i.e., RIA interneurons in the head) (Brockie et al., 2001). Using a longer promoter, we found that GLR-3 was also expressed in the intestine (Figure 1D), as well as the sensory neuron ASER (Figure 1E). The intestinal expression of GLR-3 is consistent with our finding that GLR-3 mediates cooling-evoked calcium response in the intestine. Because we are more curious about the potential role of GLR-3 in regulating sensory behavior, we decided to focus on its function in the nervous system.

The expression of GLR-3 in the sensory neuron ASER suggests that GLR-3 may regulate sensory behavior in response to cold. While ASER was originally identified as a chemosensory neuron (Ortiz et al., 2009; Pierce-Shimomura et al., 2001), the fact that GLR-3 is expressed in ASER suggests that this chemosensory neuron may also be cold-sensitive. Indeed, cooling evoked robust calcium response in ASER (Figures 2A, 2B, S2A, and S2B). *glr-3* mutant worms exhibited a severe defect in this cooling response, a phenotype that was rescued by

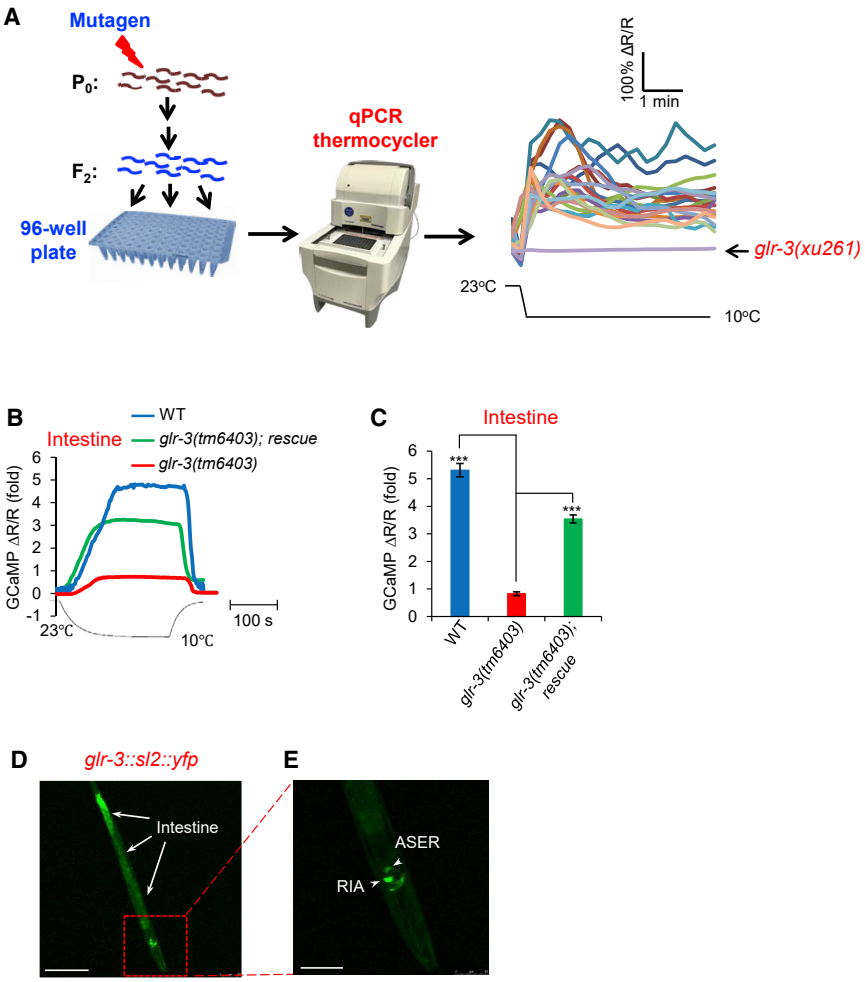

Figure 1. An Unbiased Activity-Based Genetic Screen Identifies a Key Role for GLR-3 in Cold Sensation

(A) Schematic describing the design of the screen. Worms carrying a transgene co-expressing GCaMP3 and DsRed in the intestine were mutagenized with EMS and their progeny was screened using a real-time PCR thermocycler for candidates defective in cooling-evoked calcium increase in the intestine. Sample traces were shown to the right, highlighting *glr-3*(*xu261*) mutant. The temperature was cooled from 23°C to 10°C.

(B and C) Calcium imaging shows that the *glr-3*(*tm6403*) deletion mutant exhibited a severe defect in cooling-evoked calcium response in the intestine. This phenotype was rescued by expressing wild type *glr-3* gene specifically in the intestine using the *ges-1* promoter. (B) Sample traces. (C) Bar graph. Error bars, SEM n ≥ 13. ***p < 0.0001 (ANOVA with Bonferroni test).

(D and E) *glr-3* is expressed in the intestine and the ASER sensory neuron, in addition to the central interneuron RIA. A genomic DNA fragment encompassing 3.2 kb of 5′UTR and the entire coding region of *glr-3* was used to drive YFP expression. (D) Low magnification image. (E) High magnification image highlighting neuronal expression in the head. (D) and (E) are two independent images taken with different objectives. Arrow heads point to ASER and RIAR (RIAL not visible on this focal plane). Scale bars, 100 μm (D); 20 μm (E).

See also Figure S1.

transgenic expression of wild type *glr-3* gene in ASER using an ASER-specific promoter (Figures 2A and 2B). By contrast, loss of GLR-3 did not affect salt-evoked (NaCl) calcium response in ASER neuron (Figures 2C and 2D), indicating that the chemosensory function of ASER neuron was not compromised in *glr-3* mutant worms. As a control, *che-2* mutant worms, which are known to be defective in chemosensation (Perkins et al., 1986), showed a severe defect in salt-evoked calcium transients in ASER (Figures 2C and 2D). Thus, GLR-3 acts in ASER neuron to mediate cold sensation. These results suggest that ASER is a cold-sensitive neuron.

Nevertheless, it remains possible that the observed cooling-evoked response in ASER neuron might arise from another sensory neuron (or neurons) via neurotransmission cell-non-autonomously. To exclude this possibility, we repeated the calcium imaging experiment in *unc-13* and *unc-31* mutant backgrounds, in which secretion of neurotransmitters and neuropeptides from synaptic vesicles (SV) and dense-core vesicles (DCV) is abolished, respectively (Richmond et al., 1999; Speese et al., 2007). Cooling-evoked calcium response in ASER neuron persisted in *unc-13* and *unc-31* mutant worms (Figures 2E and 2F). Thus, ASER neuron can sense cold without inputs from other neurons, providing further evidence supporting that ASER is a cold-sensitive neuron.

As GLR-3 is a member of the glutamate receptor family, we also examined mutant worms lacking *eat-4*, a gene that encodes the sole vesicular glutamate transporter in the worm genome (Lee et al., 1999). *eat-4* mutant worms, which are devoid of glutamate signaling, displayed normal cooling-evoked response in ASER neuron (Figures 2E and 2F), providing additional evidence that ASER is a cold-sensitive neuron. This experiment also demonstrates that the role of GLR-3 in ASER cold sensation is independent of its function as a glutamate receptor.

GLR-3 Acts in ASER Neuron to Mediate Cold-Avoidance Behavior

What would be the behavioral consequences following GLR-3-mediated activation of ASER neuron by cold? Activation of ASER neuron is known to trigger backward movement (reversals) followed by turns, a type of avoidance response (Suzuki et al., 2008). We first used a swimming assay to quantify turns. We found that cooling triggered turns in wild type worms (Figure 2G). *glr-3* mutant worms exhibited a severe defect in this cold-avoidance behavior (Figure 2G), while no such defect was detected in *trpa-1* mutant worms (Figure S2G). Transgenic expression of wild type *glr-3* gene specifically in ASER neuron rescued this behavioral phenotype (Figure 2G). By contrast, *glr-3* mutant worms exhibited normal salt chemotaxis behavior compared to

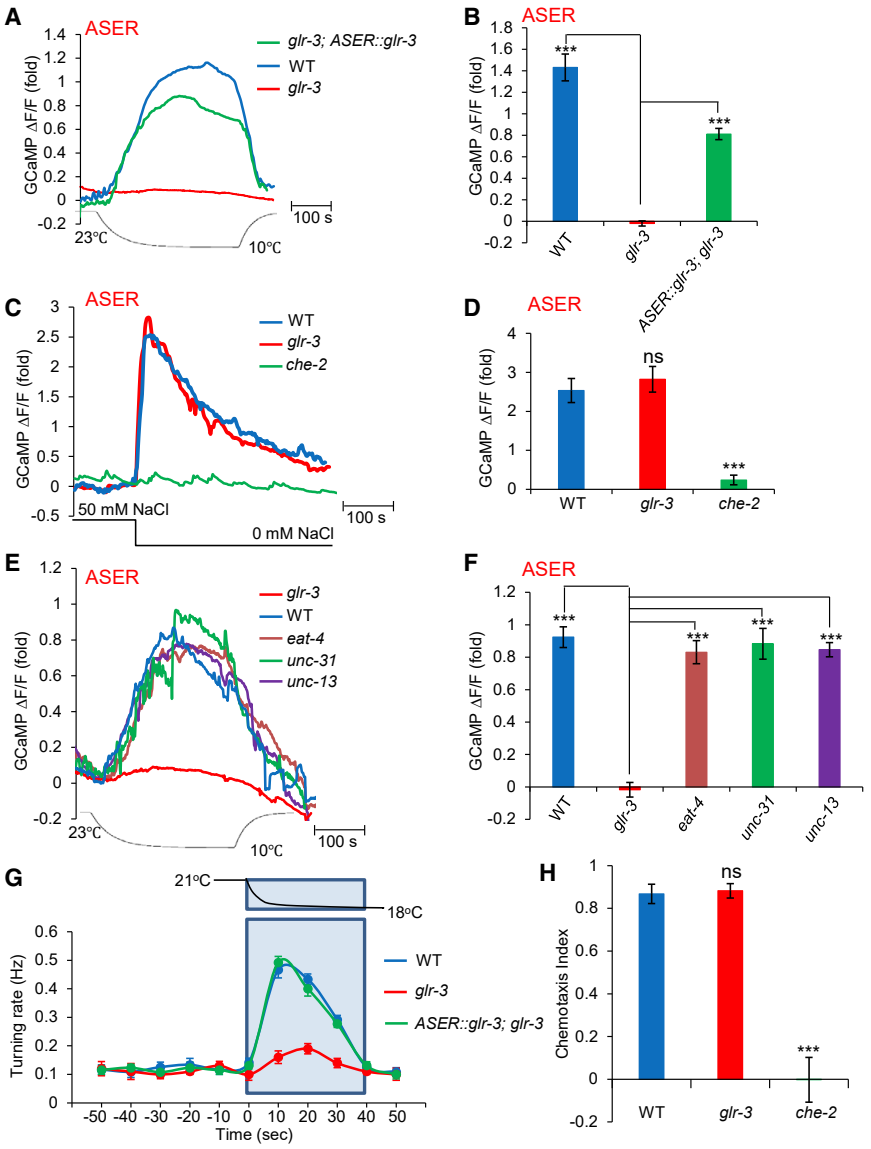

Figure 2. GLR-3 Acts in ASER Neuron to Mediate Cold Sensation and Cold-Avoidance Behavior

(A and B) ASER neuron is cold-sensitive and requires GLR-3 for cold sensation. Cooling evoked robust calcium response in ASER neuron, which is defective in *glr-3*(*tm6403*) mutant worms. Transgenic expression of wild type *glr-3* cDNA in ASER using the ASER-specific *gcy-5* promoter rescued the mutant phenotype. (A) Sample traces. (B) Bar graph. Error bars, SEM n ≥ 12. ***p < 0.0001 (ANOVA with Bonferroni test).

(C and D) Loss of GLR-3 does not affect the sensitivity of ASER neuron to salt. *glr-3*(*tm6403*) mutant worms showed normal response to NaCl gradient compared to WT, while *che-2*(*e1033*) mutant worms were defective in this response. (C) Sample traces. (B) Bar graph. Error bars, SEM n ≥ 11. ***p < 0.0001 (ANOVA with Bonferroni test).

(E and F) Cooling-evoked calcium response persists in *unc-13*, *unc-31*, and *eat-4* mutant backgrounds. (E) Sample traces. (F) Bar graphs. Error bars, SEM n ≥11. ***p < 0.0001 (ANOVA with Bonferroni test).

(G) GLR-3 mediates cooling-evoked avoidance behavior in ASER neuron. Cooling triggered turns in worms during swimming, and *glr-3* mutant worms showed a strong defect in this behavioral response, which was rescued by transgenic expression of *glr-3* cDNA in ASER. Error bars, SEM n ≥ 15.

(H) *glr-3*(*tm6403*) mutant worms show normal salt chemotaxis behavior, while *che-2*(*e1033*) mutant worms are defective in this behavior. The chemotaxis assay was run in triplicates, and the experiment was repeated four times. Error bars: SEM. ***p < 0.0001 (ANOVA with Bonferroni test).

See also Figure S2.

wild type worms, though *che-2* mutant worms were severely defective (Figure 2H). To provide additional evidence, we sought to develop another cold-avoidance behavioral assay. We examined whether cold stimuli can trigger avoidance response in worms crawling on the surface of an agar plate by cooling the air near the worm head with a cold probe. Indeed, cooling triggered backward movement (reversals) in wide-type worms (Figure S2H), and this avoidance behavioral response was defective in *glr-3* mutant worms, a phenotype that was rescued by transgenic expression of wild type *glr-3* gene specifically in ASER neuron (Figure S2H). As the swimming assay allows us to deliver cold stimuli to the worm with greater ease, we decided to focus on this assay for further characterizations. These behavioral data, together with calcium imaging results, demonstrate that GLR-3 acts in ASER sensory neuron to mediate cold sensation *in vivo*, suggesting GLR-3 as a cold receptor.

GLR-3 Can Function as a Cold Receptor

While our data show that GLR-3 is required for cold sensation *in vivo*, they do not constitute sufficient evidence supporting that GLR-3 is a cold receptor, as the observed effect might be indirect, which could potentially be contributed by a different protein. To demonstrate that a candidate protein can function as a cold receptor, one of the most commonly employed approaches is to express it in cold-insensitive heterologous cells to test whether it can confer cold sensitivity to these otherwise cold-insensitive cells (Bandell et al., 2007; Castillo et al., 2018). To this end, we first ectopically expressed GLR-3 in worm body-wall muscle cells that are commonly used as a vehicle to express exogenous proteins, particularly membrane receptors (Gong et al., 2016; Wang et al., 2012b). While body-wall muscle cells were insensitive to cold, ectopic expression of GLR-3 in muscle cells conferred cold sensitivity to these otherwise cold-insensitive cells (Figures 3A, 3B, S2C, and S2D), providing strong evidence that GLR-3 is sufficient to function as a cold receptor.

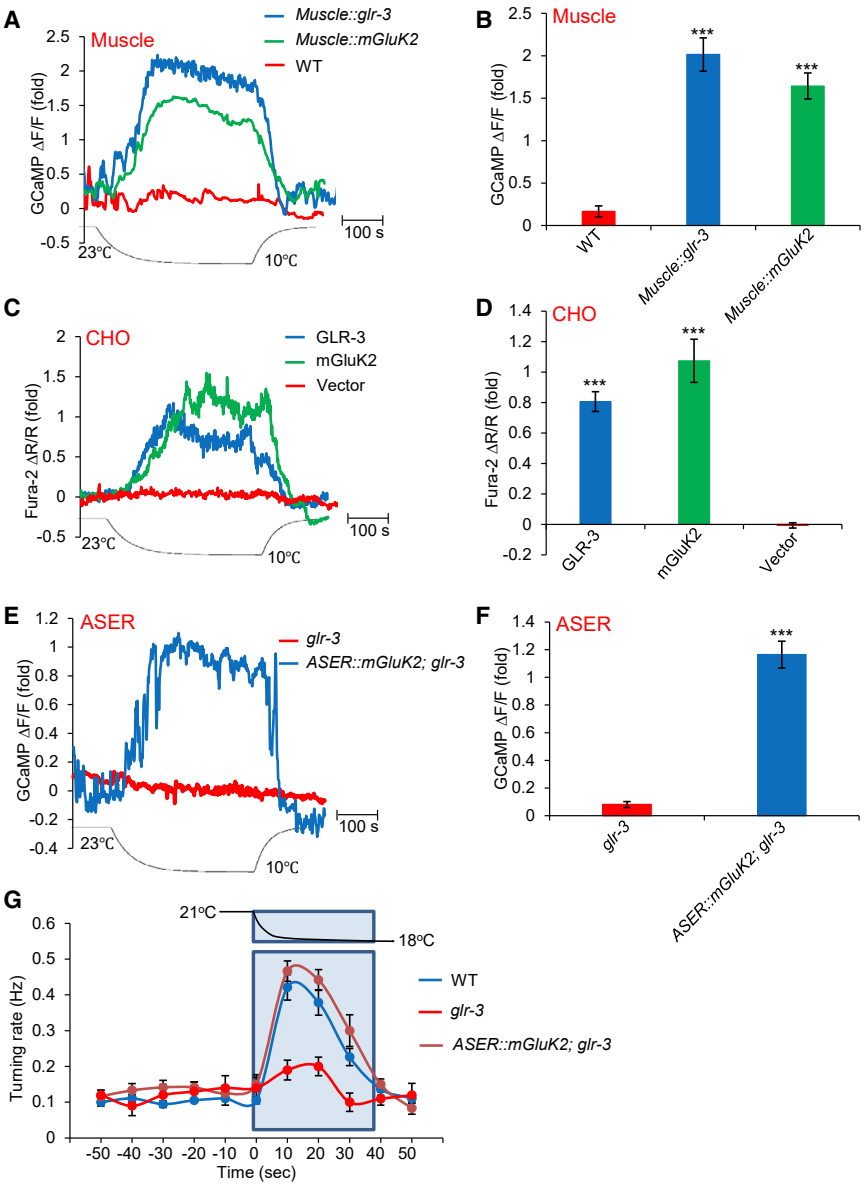

Figure 3. GLR-3 and Mouse GluK2 Function as a Cold Senor *In Vitro*, and Mouse GluK2 Can Functionally Substitute for GLR-3 in Cold Sensation *In Vivo*

(A and B) Ectopic expression of GLR-3 and mouse GluK2 in worm muscle cells confers cold-sensitivity to these cells. GLR-3 and mouse GluK2 were expressed as a transgene in worm body-wall muscles using the *myo-3* promoter. Cooling evoked calcium response in muscle cells of transgenic worms. All genotypes carried a transgene expressing GCaMP6. (A) Sample traces. (B) Bar graph. Error bars, SEM n ≥ 11. ***p < 0.0001 (ANOVA with Bonferroni test).

(C and D) Heterologous expression of GLR-3 and mouse GluK2 in CHO cells confers cold sensitivity to these cells. GLR-3 and mouse GluK2 were transfected into CHO cells, and cooling evoked calcium response in these cells as shown by Fura-2 imaging. (C) Sample traces. (D) Bar graph. Error bars, SEM n ≥ 20. ***p < 0.0001 (ANOVA with Bonferroni test).

(E and F) Mouse GluK2 can functionally substitute for GLR-3 in cold sensation in ASER neuron. Transgenic expression of mouse GluK2 in ASER neuron of *glr-3* mutant worms rescued the *glr-3* mutant phenotype in cooling-evoked calcium response in ASER neuron. (E) Sample traces. (F) Bar graph. Error bars, SEM n ≥ 12. ***p < 0.0001 (ANOVA with Bonferroni test).

(G) Mouse GluK2 can functionally substitute for GLR-3 in cold-avoidance behavior mediated by ASER neuron. Transgenic expression of mouse GluK2 in ASER neuron of *glr-3* mutant worms rescued the *glr-3* mutant phenotype in cooling-evoked avoidance behavior. Error bars, SEM n ≥ 15. See also Figures S2 and S3.

To gather further evidence, we expressed GLR-3 in mammalian cell lines. Transfection of GLR-3 in CHO cells conferred cold sensitivity to these cells (Figures 3C, 3D, S2E, and S2F). Transfection of GLR-3 in COS-7 and HeLa cells also yielded a similar result (Figures S3A–S3D). These heterologous expression data provide further evidence that GLR-3 can function as a cold receptor.

The Mouse GLR-3 Homolog GluK2 Can Functionally Substitute for Worm GLR-3 *In Vivo* and Function as a Cold Receptor *In Vitro*

Having characterized GLR-3 both *in vivo* and *in vitro*, we then wondered if the role of GLR-3 in cold sensation is evolutionarily conserved. In mouse, GluK2 is a close homolog of GLR-3 and is also a kainate-type glutamate receptor. We expressed mouse GluK2 as a transgene in ASER neuron and found that mouse GluK2 can restore cooling-evoked calcium response in ASER neuron of *glr-3* mutant worms (Figures 3E and 3F). In addition, mouse GluK2 expression in ASER also rescued the cold-avoidance behavioral phenotype in *glr-3* mutant worms (Figure 3G). Thus, mouse GluK2 can functionally substitute for GLR-3 in cold sensation *in vivo*, suggesting that mouse GluK2 has the potential to function as a cold receptor.

We also expressed mouse GluK2 as a transgene in worm muscle cells, and found that it conferred cold sensitivity to these cells (Figures 3A, 3B, S2C, and S2D). Heterologous expression of mouse GluK2 in CHO cells also conferred cold sensitivity (Figures 3C, 3D, S2E, and S2F). Cooling-evoked calcium response mediated by GluK2 and GLR-3 appears to primarily result from calcium influx (Figures S3E and S3F). As was the case with GLR-3, transfection of mouse GluK2 in COS-7 cells and HeLa cells also conferred cold sensitivity to these cells (Figures S3A–S3D). For simplicity, we focused on using CHO cells as our main heterologous expression system for further characterization of GLR-3/GluK2 *in vitro*.

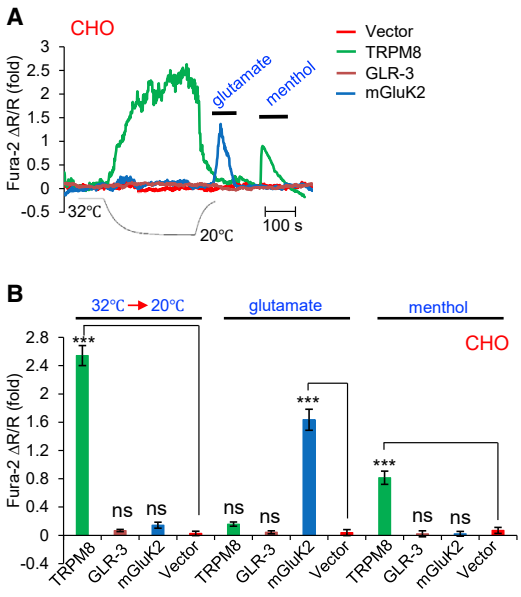

Figure 4. The Sensitivity of GLR-3/GluK2 and TRPM8 to Cold, Glutamate, and Menthol

(A and B) Cooling from 32°C to 20°C activated TRPM8 but not GLR-3 or mouse GluK2 when transfected in CHO cells. Mouse GluK2, but not GLR-3 or TRPM8, can be activated by glutamate (10 mM), while TRPM8 was also sensitive to menthol (100 μM) but not glutamate (10 mM). (A) Sample traces. (B) Bar graph. Error bars, SEM n ≥ 20. ***p < 0.0001 (ANOVA with Bonferroni test).

See also Figures S4 and S5.

In summary, heterologous expression data demonstrate that mouse GluK2 can function as a cold receptor *in vitro*, suggesting that the role of GLR-3/GluK2 as a cold receptor might be evolutionarily conserved.

GLR-3/GluK2 Mainly Senses Cold but Not Cool Temperatures

To further characterize GLR-3/GluK2, we determined its activation threshold. TRPM8 is a cool sensor with an activation threshold at ~26°C (Bandell et al., 2007; McKemy et al., 2002). Indeed, cooling from 32°C to 20°C evoked robust calcium response in CHO cells transfected with TRPM8 (Figures 4A and 4B). As TRPM8 is also a menthol receptor, we tested menthol on these cells. As predicted, menthol activated TRPM8 but not GLR-3 or mouse GluK2 in CHO cells (Figures 4A and 4B). By contrast, cooling from 32°C to 20°C triggered little, if any, calcium response in CHO cells expressing GLR-3 or mouse GluK2 (Figures 4A and 4B). This indicates that GLR-3/GluK2 was activated at a temperature much lower than TRPM8, and the activation threshold of GLR-3/GluK2 is below 20°C. Indeed, we estimated that the activation threshold for GLR-3/GluK2 in CHO cells was ~18°C (18.2 ± 0.14 for GLR-3; 18.3 ± 0.16 for mGluK2; n = 20). Similar results were obtained in ASER neuron *in vivo* (18.9 ± 0.14; n = 15; Figure S4), as well as in muscle cells ectopically expressing GLR-3 and mouse GluK2 (18.4 ± 0.16 for GLR-3; 18.5 ± 0.18 for mGluK2; n = 15). These observations together suggest GLR-3/GluK2 as a noxious cold receptor.

The Cold Sensitivity of GLR-3/GluK2 Is Independent of Its Channel Activity *In Vitro* and *In Vivo*

We made the surprising observation that while glutamate can activate mouse GluK2 in CHO cells as predicted, it cannot activate GLR-3 using the calcium imaging assay (Figures 4A and 4B). We thus recorded these CHO cells by whole-cell patch-clamping. Glutamate evoked a typical glutamate-gated current in CHO cells expressing mouse GluK2 (Figures S5D and S5I), but not GLR-3 (Figures S5H and S5I), indicating that GLR-3 lacked glutamate-gated channel activity, even though it can function as a cold receptor in these cells (Figures 3C and 3D). This surprising finding suggests that the observed cold response mediated by GLR-3/GluK2 may be independent of its channel function. To test this model, we generated two channel-dead mutants of mouse GluK2: M620R and Q622R (Figure S5A), which mutated residues adjacent to the Q/R RNA editing site in the channel pore region (Dingledine et al., 1992; Robert et al., 2002). As reported previously (Dingledine et al., 1992; Robert et al., 2002), these two point mutations abolished glutamate-gated current of mouse GluK2 in CHO cells (Figures S5E, S5F, and S5I). Strikingly, these two channel-dead GluK2 variants were still cold-sensitive in these cells (Figures 5A and 5C). Although GLR-3 lacked glutamate-gated channel activity in our assay, we introduced similar point mutations (M582R and Q584R) to disrupt any potential channel activity (Figure S5A), and found that these two channel-dead GLR-3 variants also retained normal cold sensitivity when expressed in CHO cells (Figures 5B and 5C). These results demonstrate that the cold sensitivity of GLR-3/GluK2 is independent of its channel function *in vitro*.

To obtain further evidence, we tested the two channel-dead GLR-3/GluK2 variants *in vivo*. We found that both GLR-3 and mouse GluK2 channel-dead variants can still function as a cold receptor in ASER neuron, as transgenic expression of these variants restored cooling-evoked calcium response in ASER neuron of *glr-3* mutant worms (Figures 5D–5F). Furthermore, ectopic expression of these channel-dead variants in worm muscle cells can still confer cold-sensitivity to these cells (Figures 5G–5I). We thus conclude that the cold sensitivity of GLR-3/GluK2 is independent of its channel function both *in vitro* and *in vivo*.

We also explored the converse scenario: can we identify mutations that disrupt the cold sensitivity of GLR-3/GluK2 but not its glutamate-gated channel function? The *glr-3*(*xu261*) mutant isolated from our genetic screen carried a P121L missense mutation (Figure S5B). This point mutation abolished the cold sensitivity of GLR-3 (Figures 5J and 5L). As GLR-3 did not exhibit channel activity on its own, we tested our model in mouse GluK2. Because this P residue is not found in mouse GluK2, we mutated an adjacent P residue P151 to L in the mouse protein (Figure S5B). These P residues are located in the N-terminal ATD domain of GLR-3/GluK2 (Traynelis et al., 2010). P151L mutation disrupted the cold sensitivity of mouse GluK2 in CHO cells (Figures 5K and 5L), and a corresponding P130L mutation in GLR-3 exerted a similar effect (Figures 5J and 5L). This demonstrates that the N-terminal ATD domain is required for the cold-sensitivity of GLR-3/GluK2. Strikingly, despite its lack of cold sensitivity, GluK2(P151L) retained glutamate-evoked channel activity in calcium imaging assay (Figures 5K and 5L). Whole-cell

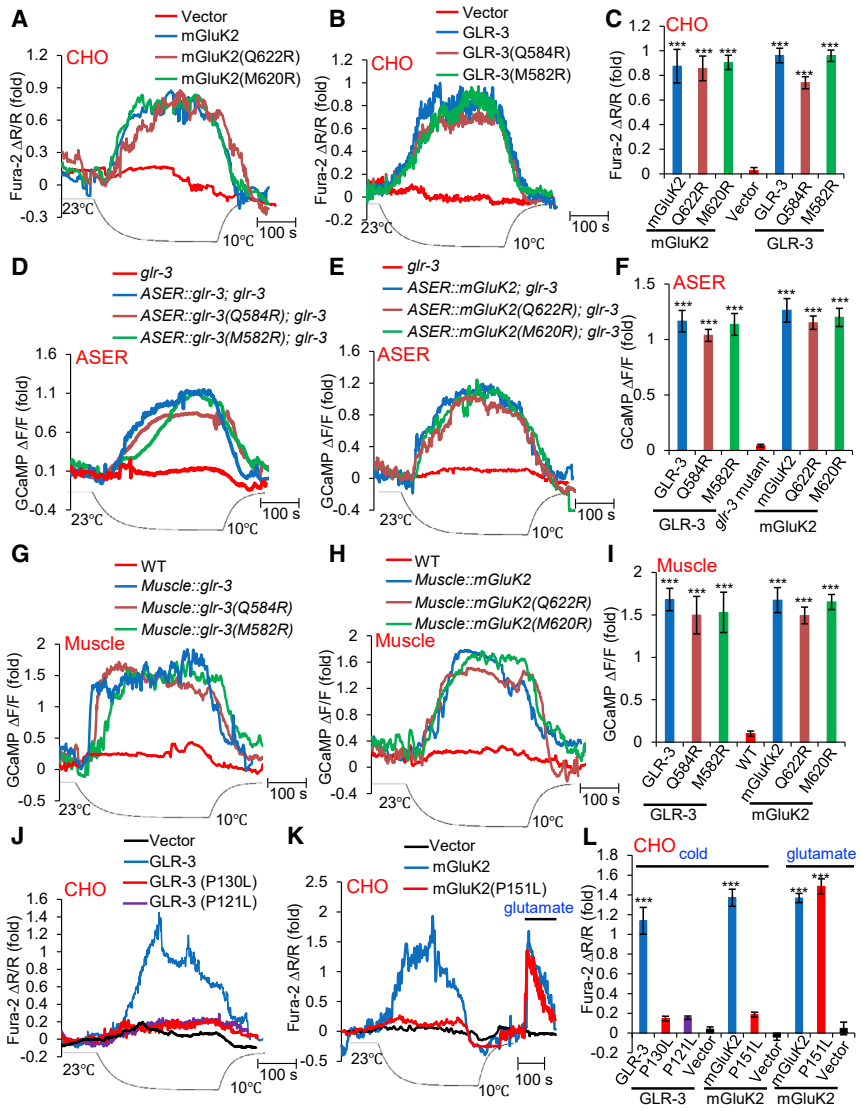

Figure 5. The Cold Sensitivity of GLR-3/GluK2 Is Independent of Its Channel Function

(A–C) Channel-dead GLR-3/GluK2 variants show normal cold sensitivity in CHO cells. The two channel-dead variants of mouse GluK2 (A), as well as GLR-3 (B), showed similar cold sensitivity compared to wild type GluK2/GLR-3 when transfected in CHO cells. (A and B) Sample traces. (C) Bar graph. Error bars, SEM n ≥ 20. ***p < 0.0001 (ANOVA with Bonferroni test).

(D–F) Channel-dead GLR-3/GluK2 variants show normal cold sensitivity in ASER neuron *in vivo*. The two channel-dead variants of GLR-3 (D), as well as mouse GluK2 (E), showed similar cold sensitivity compared to wild type GluK2/GLR-3 when expressed as a transgene in ASER neuron of *glr-3* mutant worms. (D and E) Sample traces. (F) Bar graph. Error bars, SEM n ≥ 12. ***p < 0.0001 (ANOVA with Bonferroni test).

(G–I) Channel-dead GLR-3/GluK2 variants show normal cold sensitivity in worm muscle cells. The two channel-dead variants of GLR-3 (G), as well as mouse GluK2 (H), showed similar cold sensitivity compared to wild type GluK2/GLR-3 when expressed as a transgene in worm muscle cells. (G and H) Sample traces. (I) Bar graph. Error bars, SEM n ≥ 12. ***p < 0.0001 (ANOVA with Bonferroni test).

(J–L) Cold-insensitive GLR-3/GluK2 mutants display glutamate-gated channel activity. (J) GLR-3(P121L) and GLR-3(P130L) were no longer sensitive to cold. (K) GluK2(P151L) was insensitive to cold but sensitive to glutamate. (L) Bar graph. Error bars, SEM n ≥ 22. ***p < 0.0001 (ANOVA with Bonferroni test).

See also Figure S5.

recording also showed that GluK2(P151L) retained glutamate-gated current, although its kinetics were altered (Figures S5G and S5I). This is consistent with the notion that the ATD domain of glutamate receptors is not required for their channel function and only plays a modulatory role (Traynelis et al., 2010). Thus, it appears that the cold-sensing and glutamate-gated channel functions of GLR-3/GluK2 can be dissociated and may require distinct domains. Together, our results suggest that GLR-3/GluK2 may function as a receptor-type cold sensor rather than a cold-activated channel.

GLR-3/GluK2 Functions as a Metabotropic Cold Receptor and Requires G Protein Signaling to Transmit Cold Signals *In Vitro* and *In Vivo*

Interestingly, mammalian kainate receptors have been reported to possess both metabotropic and ionotropic functions (Rodríguez-Moreno and Lerma, 1998; Rozas et al., 2003; Valbuena and Lerma, 2016). When acting as metabotropic receptors, they transmit glutamate signals via G proteins (Rodríguez-Moreno and Lerma, 1998; Rozas et al., 2003; Valbuena and Lerma, 2016). In this case, these kainate receptors act as "GPCR-like" glutamate receptors rather than glutamate-gated channels (Rodríguez-Moreno and Lerma, 1998; Rozas et al., 2003; Valbuena and Lerma, 2016). This led us to hypothesize that GLR-3/GluK2 may also function as a "GPCR-like" cold receptor. If so, GLR-3/GluK2 should depend on G proteins to transmit cold signals. To test this, we examined mSIRK, a membrane-permeable peptide that dissociates Gα from Gβγ without stimulating its GTP-binding activity, thereby inhibiting receptor-mediated activation of G proteins (Goubaeva et al., 2003). mSIRK abolished cooling-evoked calcium response in CHO cells expressing GLR-3 or mouse GluK2 (Figures 6A–6D). Pertussis toxin (PTX), a Gi/o inhibitor (Gierschik, 1992), also blocked the cold sensitivity of GLR-3 and mouse GluK2 in CHO cells (Figures 6A–6D). By contrast, the Gq/11 inhibitor, YM-254890 (Takasaki et al., 2004), had no effect on the cold sensitivity of GLR-3/GluK2 (Figures 6A–6D). As a control, this Gq/11 inhibitor can block bradykinin-evoked calcium response (Figures S6A and S6B), which was mediated by endogenous Gq/11-coupled bradykinin receptors in CHO cells (Pauwels and Colpaert, 2003),

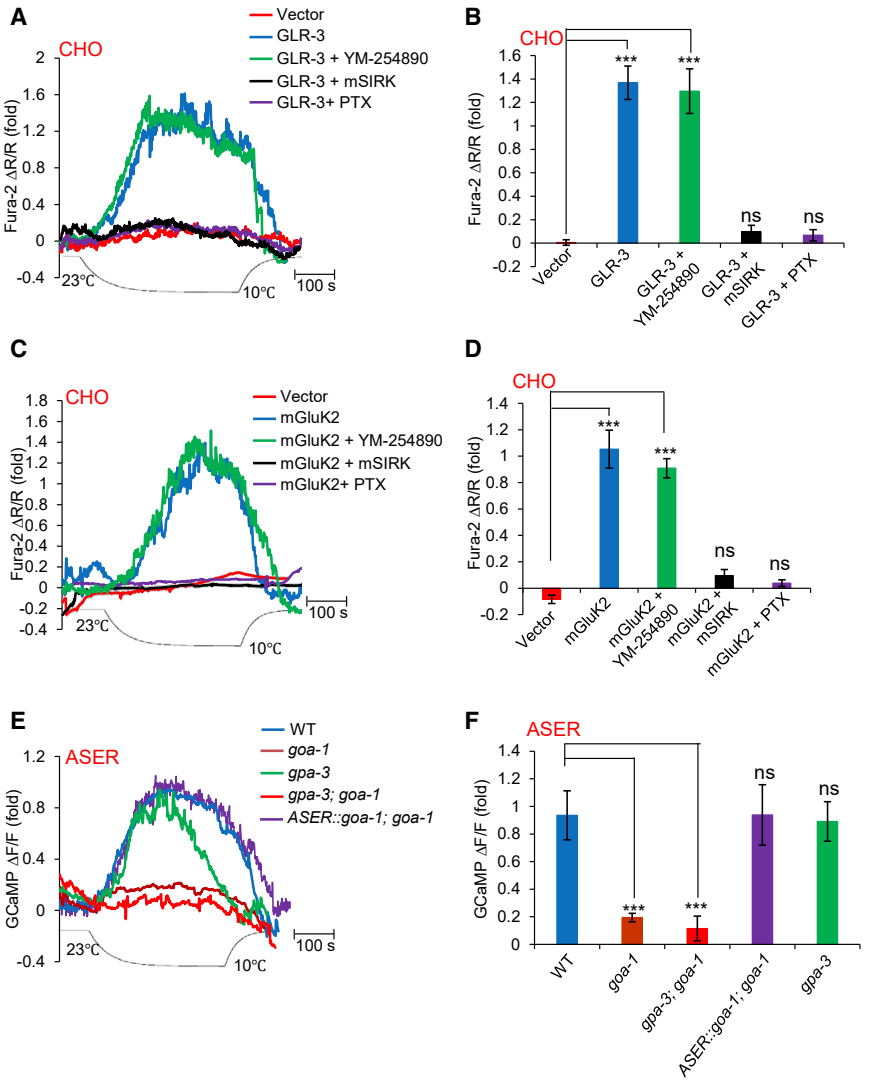

Figure 6. GLR-3 Relies on G Protein Signaling to Transmit Cold Signals

(A and B) G protein inhibitors blocked the cold sensitivity of GLR-3 in CHO cells. The pan-G protein inhibitor mSIRK (50 μM), the Gi/o inhibitor PTX (100 ng/mL), but not the Gq/11 inhibitor YM-254890 (10 μM), blocked cooling-evoked calcium response mediated by GLR-3 in CHO cells. (A) Sample traces. (B) Bar graph. Error bars, SEM n ≥ 20. ***p < 0.0001 (ANOVA with Bonferroni test).

(C and D) G protein inhibitors blocked the cold sensitivity of mouse GluK2 in CHO cells. The pan-G protein inhibitor mSIRK (50 μM), the Gi/o inhibitor PTX (100 ng/mL), but not the Gq/11 inhibitor YM-254890 (10 μM), blocked cooling-evoked calcium response mediated by mouse GluK2 in CHO cells. (C) Sample traces. (D) Bar graph. Error bars, SEM n ≥ 20. ***p < 0.0001 (ANOVA with Bonferroni test).

(E and F) The cold sensitivity of ASER neuron requires the Gi/o protein gene *goa-1*. *goa-1*(*n1134*) mutant worms showed a strong defect in cooling-evoked calcium response in ASER neuron, a phenotype that was rescued by transgenic expression of wild type *goa-1* gene specifically in ASER neuron. (E) Sample traces. (F) Bar graph. Error bars, SEM n ≥ 11. ***p < 0.0001 (ANOVA with Bonferroni test).

See also Figure S6.

whereas the Gi/o inhibitor PTX had no effect on bradykinin-evoked response (Figures S6A and S6B). These results demonstrate that GLR-3/GluK2 transmits cold signals via Gi/o signaling *in vitro*.

Encouraged by our *in vitro* results, we next tested whether GLR-3 transmits cold signals via Gi/o signaling *in vivo*. ASER neuron expresses at least two Gi/o genes: *goa-1* and *gpa-3* (Jansen et al., 1999). Mutations in *goa-1*, but not *gpa-3*, led to a severe defect in cooling-evoked calcium response in ASER neuron (Figures 6E and 6F), a phenotype that was rescued by transgenic expression of wild type *goa-1* gene specifically in ASER neuron (Figures 6E and 6F), suggesting that GLR-3 transmits cold signals via Gi/o signaling *in vivo*. A similar result was obtained with cooling-evoked calcium response in the intestine (Figures S6C and S6D). Taken together, both of our *in vitro* and *in vivo* results support the model that GLR-3/GluK2 functions as a metabotropic, rather than an ionotropic, cold receptor, and does so by transmitting cold signals via Gi/o proteins. This identifies GLR-3/GluK2 as a previously unknown type of cold receptor.

Mouse DRG Neurons Express GluK2 and Knockdown of GluK2 in DRG Neurons Suppresses Their Sensitivity to Cold but Not Cool Temperatures

Mammalian glutamate receptors are best known to function in the brain to regulate synaptic transmission and plasticity. Interestingly, some of these receptors are also expressed in the peripheral nervous system such as DRG sensory neurons but with an unknown function (Coggeshall and Carlton, 1998; Huettner, 1990). We thus wondered if GluK2 is expressed in DRG neurons. These primary sensory neurons detect somatosensory and painful stimuli in the periphery, including temperature cues. Using RNAscope assay, we detected GluK2 mRNA transcripts in mouse DRGs (Figures 7A and 7B). Approximately 13.6% (140/1031) DRG neurons expressed GluK2. Among them, most were small-diameter neurons (75.0%, 105/140), while a small percentage (24.2%, 34/140) were medium-diameter neurons. This data suggests that GluK2 is expressed in DRG neurons.

We next knocked down GluK2 expression in cultured DRG neurons with siRNA (Figure 7C). While knockdown of GluK2 did not affect the sensitivity of DRG neurons to cool temperatures (cooling to 22°C) (Figures 7D and 7F; 30/699 control cells versus 26/598 siRNA cells responded), it greatly reduced the sensitivity of these sensory neurons to cold temperatures (cooling to 10°C) (Figures 7E and 7F; 131/699 control cells versus

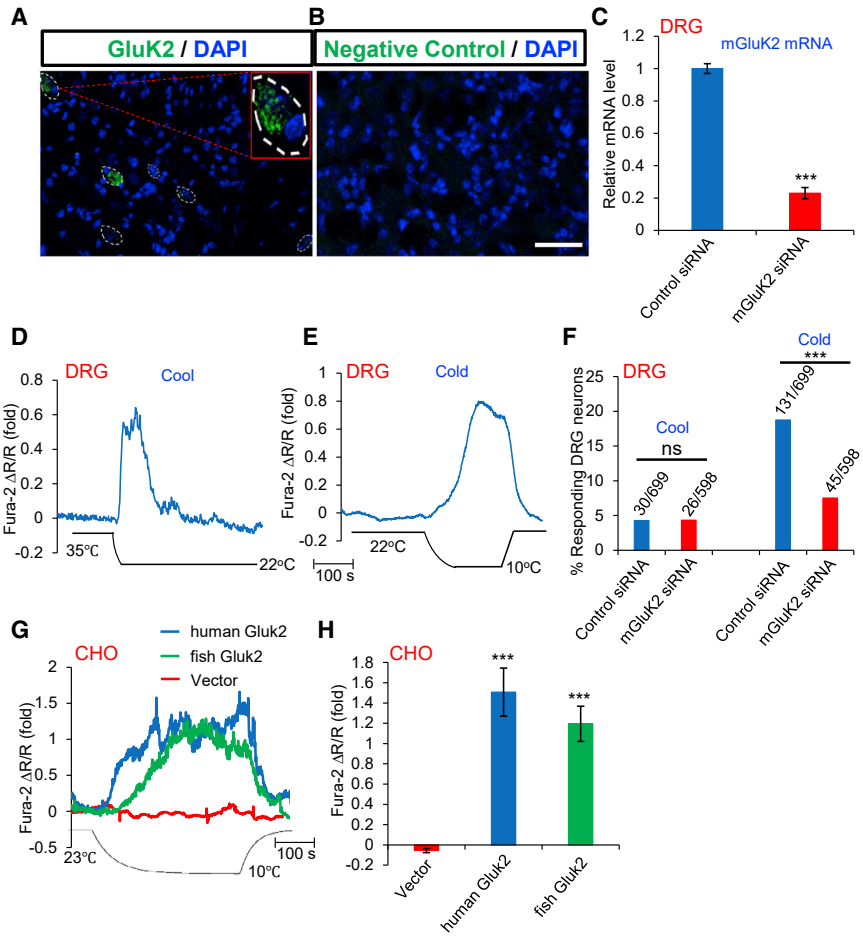

Figure 7. Mouse DRG Neurons Express GluK2 and Knockdown of GluK2 in DRG Neurons Suppresses Their Sensitivity to Cold but Not Cool Temperatures

(A and B) Mouse DRG neurons express GluK2 mRNA transcripts. (A) *In situ* hybridization using RNAscope assay detected GluK2 mRNA signals (puncta) in DRG tissue. The dotted ovals denote the shape of the soma of the neurons expressing GluK2 transcripts. Only those neurons with at least 4 puncta inside the soma were scored positive, as the background signals detected by the control probe varied between 0–2 puncta/cell. The inset image in (A) highlights one GluK2-positive neuron. Green, GluK2 transcripts. Blue, DAPI. (B) Negative control probe staining (provided by Advanced Cell Diagnostics). Scale bar, 50 μm.

(C) Real-time qPCR analysis shows that siRNA knockdown of GluK2 in mouse DRG neurons greatly reduced the mRNA level of GluK2. qPCR reactions were run in triplicates. The experiment was repeated five times. Error bars, SEM. ***$p < 0.0001$ (t test).

(D–F) siRNA knockdown of GluK2 in mouse DRG neurons greatly reduces the sensitivity of these neurons to cold but not cool temperatures. (D) Sample trace showing calcium response to cool temperature (cooling to 22°C). (E) Sample trace showing calcium response to cold temperature (cooling to 10°C). (F) Bar graph. Sample sizes were shown on top of each bar. ***$p < 0.0001$ (χ^2 test).

(G and H) Fish and human GluK2 can also function as a cold receptor *in vitro*. Heterologous expression of fish and human GluK2 in CHO cells confers cold sensitivity to these cells. (G) Sample traces. (H) Bar graph. Error bars, SEM n ≥ 20. ***$p < 0.0001$ (ANOVA with Bonferroni test).

45/598 siRNA cells responded; χ^2 test, $p < 0.0001$). This is consistent with our data that GluK2 primarily senses cold but not cool temperatures. These observations suggest that GluK2 may sense cold temperatures in mouse DRG neurons.

The Fish and Human GLR-3/GluK2 Homologs Can Also Function as a Cold Receptor *In Vitro*

Our observation that both GLR-3 and mouse GluK2 can function as a cold receptor prompted us to ask how deeply the role of GLR-3/GluK2 as a cold receptor is conserved across the phylogeny. We thus tested the zebrafish and human homologs of GluK2. Transfection of both zebrafish and human GluK2 in CHO cells conferred cold sensitivity to these cells (Figures 7G and 7H), suggesting that they both can function as a cold receptor in heterologous systems. Thus, GLR-3/GluK2 from worms, zebrafish, mice, and humans all have the capacity to function as a cold receptor, suggesting that the function of GLR-3/GluK2 in cold sensation might be evolutionarily conserved from worms to humans.

DISCUSSION

Despite decades of intensive research, little is known about the molecular mechanisms underlying cold sensation. Previous efforts to identify cold sensors using candidate gene approaches have not been very fruitful, although this approach is highly successful in identifying heat sensors such as thermo-TRP channels (Bandell et al., 2007; Castillo et al., 2018). To overcome this technical difficulty, in the current study, we designed an unbiased, activity-based genetic screen for cold-sensing receptors in *C. elegans* using a real-time PCR thermocycler. We showed that GLR-3, a member of the kainate-type of glutamate receptors, surprisingly functions as a cold receptor.

GLR-3 possesses several interesting features. First, its activation threshold is lower than that of TRPM8 (i.e., ~18°C versus ~26°C), which is close to the range of noxious cold, suggesting that GLR-3 may primarily sense noxious cold rather than cool temperatures. Second, unlike other thermal receptors that are temperature-gated ion channels (Bandell et al., 2007; Castillo et al., 2018), GLR-3 functions as a metabotropic thermal receptor. This is supported by the observation that channel-dead GLR-3 and mouse GluK2 variants show normal cold sensitivity. In addition, although worm GLR-3 is cold-sensitive, it does not display any detectable channel activity. Furthermore, both GLR-3 and mouse GluK2 rely on G proteins to transmit cold signals. Another interesting feature of GLR-3 is that glutamate is not required for this receptor to sense cold *in vivo*, as *eat-4* mutant

worms, which are devoid of glutamate signaling, show normal cold sensitivity in ASER neuron. GLR-3 and mouse GluK2 can also sense cold in the absence of glutamate in heterologous systems. This suggests that the cold-sensing activity of GLR-3/GluK2 is independent of its glutamate receptor function. Furthermore, mutations in the N-terminal ATD domain of GluK2, which disrupt the cold sensitivity of mouse GluK2, spare its glutamate-gated channel activity, suggesting that the functions of cold-sensing and glutamate-sensing of GluK2 could be dissociated and may require distinct domains. We thus propose that some glutamate receptors, such as GLR-3/GluK2, are multifunctional, acting as a chemical receptor in the CNS but functioning as a thermal receptor in the periphery.

As a metabotropic cold receptor, GLR-3 requires G proteins to transmit cold signals, which would presumably lead to the activation of downstream transduction channels and hence cooling-evoked calcium response. Indeed, cooling-activated calcium response mediated by GLR-3/GluK2 primarily results from calcium influx (Figures S3E and S3F), suggesting the presence of downstream transduction channel(s). The identity of the transduction channel(s) acting downstream of GLR-3 and G proteins is currently unknown. Future studies are needed to address this question, as well as to identify the detailed transduction mechanisms. We found that a Gi/o protein is required for GLR-3 to transduce cold signals. Although Gi/o is known to trigger inhibitory signaling, interestingly, it can also be coupled to excitatory signaling mediated mostly by its $G\beta\gamma$ subunits (Neves et al., 2002). Notably, in addition to channels, G proteins can also regulate many other types of effectors, such as enzymes, transporters, transcriptional machinery, mobility/contractibility machinery, secretory machinery, etc. (Neves et al., 2002). In this regard, a metabotropic thermal receptor would be more functionally versatile and may potentially regulate a wider range of cellular processes. GLR-3 thus represents a previously unknown class of thermal receptor.

Glutamate receptors are chemical-sensing receptors that are well known to mediate chemical synaptic transmission/plasticity in the CNS. Our results reveal an unexpected case where a central chemical receptor functions as a thermal receptor in the periphery. As glutamate receptors are evolutionarily conserved, this raises the intriguing possibility that in addition to sensing chemicals (i.e., glutamate), one ancestral function of glutamate receptors might be to sense non-chemical cues such as temperature. Interestingly, some insect chemical-sensing ionotropic receptors (IRs) regulate thermosensation (Budelli et al., 2019). It would be interesting to test whether they can sense temperature.

Another interesting observation is that the vertebrate GLR-3 homolog GluK2 from mouse, human, and zebrafish can all function as a cold receptor in heterologous systems. Mouse GluK2 can also functionally substitute for worm GLR-3 in cold sensation *in vivo*. In addition to the brain, we found that mouse GluK2 is expressed in DRG neurons in the periphery, and knockdown of GluK2 in DRG neurons greatly reduced the sensitivity of these primary sensory neurons to cold but not cool temperatures, raising the possibility that GluK2 may function as a cold receptor in DRG neurons in mammals. We thus propose that the role of GLR-3/GluK2 as a cold receptor may be evolutionarily conserved from worms to humans.

STAR★METHODS

Detailed methods are provided in the online version of this paper and include the following:

- KEY RESOURCES TABLE
- LEAD CONTACT AND MATERIALS AVAILABILITY
- EXPERIMENTAL MODEL AND SUBJECT DETAILS
- METHOD DETAILS
  - Molecular biology and genetics
  - Genetic screen
  - *C. elegans* calcium imaging and behavioral assays
  - Cell culture and calcium imaging
  - Mouse DRG neuron culture, transfection, qPCR, and calcium imaging
  - Mouse DRG *in situ* hybridization (RNAscope)
  - Electrophysiology
- QUANTIFICATION AND STATISTICAL ANALYSIS
- DATA AND CODE AVAILABILITY

ACKNOWLEDGMENTS

We thank Min Guo, Xi Lan, Jie Liu, Rebekah Ronan, Bonnie Zeng, Seth Kattapong-Graber, and Jonathan Ronan for technical assistance, and Bing Ye for comments. Some strains were obtained from the CGC and Japan knockout consortium. E.A.R. was supported by an NIA T32 training grant. Jianfeng Liu received funding support from the MOST and NSFC (2018YFA0507003, 31420103909, 81872945, and 81720108031) and the 111 project of the MOE (B08029). G.-H.K. received funding support from the National Research Foundation of Korea (NRF-2017R1A4A1015564). B.D. received funding support from the NINDS. X.Z.S.X. received funding support from the NIGMS and NIA.

AUTHOR CONTRIBUTIONS

J.G. and E.A.R. performed *in vivo* experiments and analyzed the data. J.G. and F.H. performed *in vitro* experiments and analyzed the data. Jinzhi Liu generated nearly all the reagents. W.C., M.F., H.L., and B.D. performed mouse DRG experiments and analyzed the data. W.Z. assisted J.G. in performing some experiments. Z.L. helped identify GLR-3 expression pattern. G.-H.K. and K.P.P. contributed to the design and fabrication of cooling devices. J.G., E.A.R., Jianfeng Liu, and X.Z.S.X. wrote the paper with input from other authors.

DECLARATION OF INTERESTS

The authors declare no competing interests.

Received: March 10, 2019
Revised: May 31, 2019
Accepted: July 17, 2019
Published: August 29, 2019

REFERENCES

Bandell, M., Macpherson, L.J., and Patapoutian, A. (2007). From chills to chilis: mechanisms for thermosensation and chemesthesis via thermoTRPs. Curr. Opin. Neurobiol. *17*, 490–497.

Bargmann, C.I. (2006). Chemosensation in C. elegans. WormBook, 1–29.

Bautista, D.M., Siemens, J., Glazer, J.M., Tsuruda, P.R., Basbaum, A.I., Stucky, C.L., Jordt, S.E., and Julius, D. (2007). The menthol receptor TRPM8 is the principal detector of environmental cold. Nature *448*, 204–208.

Bowie, D. (2008). Ionotropic glutamate receptors & CNS disorders. CNS Neurol. Disord. Drug Targets *7*, 129–143.

Brockie, P.J., Madsen, D.M., Zheng, Y., Mellem, J., and Maricq, A.V. (2001). Differential expression of glutamate receptor subunits in the nervous system of Caenorhabditis elegans and their regulation by the homeodomain protein UNC-42. J. Neurosci. *21*, 1510–1522.

Budelli, G., Ni, L., Berciu, C., van Giesen, L., Knecht, Z.A., Chang, E.C., Kaminski, B., Silbering, A.F., Samuel, A., Klein, M., et al. (2019). Ionotropic Receptors Specify the Morphogenesis of Phasic Sensors Controlling Rapid Thermal Preference in Drosophila. Neuron *101*, 738–747.

Castillo, K., Diaz-Franulic, I., Canan, J., Gonzalez-Nilo, F., and Latorre, R. (2018). Thermally activated TRP channels: molecular sensors for temperature detection. Phys. Biol. *15*, 021001.

Coggeshall, R.E., and Carlton, S.M. (1998). Ultrastructural analysis of NMDA, AMPA, and kainate receptors on unmyelinated and myelinated axons in the periphery. J. Comp. Neurol. *391*, 78–86.

Dhaka, A., Murray, A.N., Mathur, J., Earley, T.J., Petrus, M.J., and Patapoutian, A. (2007). TRPM8 is required for cold sensation in mice. Neuron *54*, 371–378.

Dingledine, R., Hume, R.I., and Heinemann, S.F. (1992). Structural determinants of barium permeation and rectification in non-NMDA glutamate receptor channels. J. Neurosci. *12*, 4080–4087.

Fang, X., Djouhri, L., McMullan, S., Berry, C., Okuse, K., Waxman, S.G., and Lawson, S.N. (2005). trkA is expressed in nociceptive neurons and influences electrophysiological properties via Nav1.8 expression in rapidly conducting nociceptors. J. Neurosci. *25*, 4868–4878.

Foulkes, T., and Wood, J.N. (2007). Mechanisms of cold pain. Channels (Austin) *1*, 154–160.

Garrity, P.A., Goodman, M.B., Samuel, A.D., and Sengupta, P. (2010). Running hot and cold: behavioral strategies, neural circuits, and the molecular machinery for thermotaxis in C. elegans and Drosophila. Genes Dev. *24*, 2365–2382.

Gierschik, P. (1992). ADP-ribosylation of signal-transducing guanine nucleotide-binding proteins by pertussis toxin. Curr. Top. Microbiol. Immunol. *175*, 69–96.

Gong, J., Yuan, Y., Ward, A., Kang, L., Zhang, B., Wu, Z., Peng, J., Feng, Z., Liu, J., and Xu, X.Z. (2016). The C. elegans Taste Receptor Homolog LITE-1 Is a Photoreceptor. Cell *167*, 1252–1263.

Goodman, M.B. (2006). Mechanosensation. WormBook, 1–14.

Goubaeva, F., Ghosh, M., Malik, S., Yang, J., Hinkle, P.M., Griendling, K.K., Neubig, R.R., and Smrcka, A.V. (2003). Stimulation of cellular signaling and G protein subunit dissociation by G protein betagamma subunit-binding peptides. J. Biol. Chem. *278*, 19634–19641.

Huettner, J.E. (1990). Glutamate receptor channels in rat DRG neurons: activation by kainate and quisqualate and blockade of desensitization by Con A. Neuron *5*, 255–266.

Jansen, G., Thijssen, K.L., Werner, P., van der Horst, M., Hazendonk, E., and Plasterk, R.H. (1999). The complete family of genes encoding G proteins of Caenorhabditis elegans. Nat. Genet. *21*, 414–419.

Lee, R.Y., Sawin, E.R., Chalfie, M., Horvitz, H.R., and Avery, L. (1999). EAT-4, a homolog of a mammalian sodium-dependent inorganic phosphate cotransporter, is necessary for glutamatergic neurotransmission in caenorhabditis elegans. J. Neurosci. *19*, 159–167.

Lou, S., Duan, B., Vong, L., Lowell, B.B., and Ma, Q. (2013). Runx1 controls terminal morphology and mechanosensitivity of VGLUT3-expressing C-mechanoreceptors. J. Neurosci. *33*, 870–882.

McGhee, J.D. (2007). The C. elegans intestine. WormBook, 1–36.

McKemy, D.D., Neuhausser, W.M., and Julius, D. (2002). Identification of a cold receptor reveals a general role for TRP channels in thermosensation. Nature *416*, 52–58.

Minevich, G., Park, D.S., Blankenberg, D., Poole, R.J., and Hobert, O. (2012). CloudMap: a cloud-based pipeline for analysis of mutant genome sequences. Genetics *192*, 1249–1269.

Moparthi, L., Kichko, T.I., Eberhardt, M., Högestätt, E.D., Kjellbom, P., Johanson, U., Reeh, P.W., Leffler, A., Filipovic, M.R., and Zygmunt, P.M. (2016). Human TRPA1 is a heat sensor displaying intrinsic U-shaped thermosensitivity. Sci. Rep. *6*, 28763.

Neves, S.R., Ram, P.T., and Iyengar, R. (2002). G protein pathways. Science *296*, 1636–1639.

Ortiz, C.O., Faumont, S., Takayama, J., Ahmed, H.K., Goldsmith, A.D., Pocock, R., McCormick, K.E., Kunimoto, H., Iino, Y., Lockery, S., and Hobert, O. (2009). Lateralized gustatory behavior of C. elegans is controlled by specific receptor-type guanylyl cyclases. Curr. Biol. *19*, 996–1004.

Pauwels, P.J., and Colpaert, F.C. (2003). Ca2+ responses in Chinese hamster ovary-K1 cells demonstrate an atypical pattern of ligand-induced 5-HT1A receptor activation. J. Pharmacol. Exp. Ther. *307*, 608–614.

Peier, A.M., Moqrich, A., Hergarden, A.C., Reeve, A.J., Andersson, D.A., Story, G.M., Earley, T.J., Dragoni, I., McIntyre, P., Bevan, S., and Patapoutian, A. (2002). A TRP channel that senses cold stimuli and menthol. Cell *108*, 705–715.

Perkins, L.A., Hedgecock, E.M., Thomson, J.N., and Culotti, J.G. (1986). Mutant sensory cilia in the nematode Caenorhabditis elegans. Dev. Biol. *117*, 456–487.

Pierce-Shimomura, J.T., Faumont, S., Gaston, M.R., Pearson, B.J., and Lockery, S.R. (2001). The homeobox gene lim-6 is required for distinct chemosensory representations in C. elegans. Nature *410*, 694–698.

Richmond, J.E., Davis, W.S., and Jorgensen, E.M. (1999). UNC-13 is required for synaptic vesicle fusion in C. elegans. Nat. Neurosci. *2*, 959–964.

Robert, A., Hyde, R., Hughes, T.E., and Howe, J.R. (2002). The expression of dominant-negative subunits selectively suppresses neuronal AMPA and kainate receptors. Neuroscience *115*, 1199–1210.

Rodríguez-Moreno, A., and Lerma, J. (1998). Kainate receptor modulation of GABA release involves a metabotropic function. Neuron *20*, 1211–1218.

Rozas, J.L., Paternain, A.V., and Lerma, J. (2003). Noncanonical signaling by ionotropic kainate receptors. Neuron *39*, 543–553.

Schepers, R.J., and Ringkamp, M. (2010). Thermoreceptors and thermosensitive afferents. Neurosci. Biobehav. Rev. *34*, 177–184.

Speese, S., Petrie, M., Schuske, K., Ailion, M., Ann, K., Iwasaki, K., Jorgensen, E.M., and Martin, T.F. (2007). UNC-31 (CAPS) is required for dense-core vesicle but not synaptic vesicle exocytosis in Caenorhabditis elegans. J. Neurosci. *27*, 6150–6162.

Story, G.M., Peier, A.M., Reeve, A.J., Eid, S.R., Mosbacher, J., Hricik, T.R., Earley, T.J., Hergarden, A.C., Andersson, D.A., Hwang, S.W., et al. (2003). ANKTM1, a TRP-like channel expressed in nociceptive neurons, is activated by cold temperatures. Cell *112*, 819–829.

Suzuki, H., Thiele, T.R., Faumont, S., Ezcurra, M., Lockery, S.R., and Schafer, W.R. (2008). Functional asymmetry in Caenorhabditis elegans taste neurons and its computational role in chemotaxis. Nature *454*, 114–117.

Takasaki, J., Saito, T., Taniguchi, M., Kawasaki, T., Moritani, Y., Hayashi, K., and Kobori, M. (2004). A novel Galphaq/11-selective inhibitor. J. Biol. Chem. *279*, 47438–47445.

Tomioka, M., Adachi, T., Suzuki, H., Kunitomo, H., Schafer, W.R., and Iino, Y. (2006). The insulin/PI 3-kinase pathway regulates salt chemotaxis learning in Caenorhabditis elegans. Neuron *51*, 613–625.

Traynelis, S.F., Wollmuth, L.P., McBain, C.J., Menniti, F.S., Vance, K.M., Ogden, K.K., Hansen, K.B., Yuan, H., Myers, S.J., and Dingledine, R. (2010). Glutamate receptor ion channels: structure, regulation, and function. Pharmacol. Rev. *62*, 405–496.

Valbuena, S., and Lerma, J. (2016). Non-canonical Signaling, the Hidden Life of Ligand-Gated Ion Channels. Neuron *92*, 316–329.

Vandewauw, I., De Clercq, K., Mulier, M., Held, K., Pinto, S., Van Ranst, N., Segal, A., Voet, T., Vennekens, R., Zimmermann, K., et al. (2018). A TRP channel trio mediates acute noxious heat sensing. Nature *555*, 662–666.

Wang, F., Flanagan, J., Su, N., Wang, L.C., Bui, S., Nielson, A., Wu, X., Vo, H.T., Ma, X.J., and Luo, Y. (2012a). RNAscope: a novel in situ RNA analysis platform for formalin-fixed, paraffin-embedded tissues. J. Mol. Diagn. *14*, 22–29.

Wang, R., Mellem, J.E., Jensen, M., Brockie, P.J., Walker, C.S., Hoerndli, F.J., Hauth, L., Madsen, D.M., and Maricq, A.V. (2012b). The SOL-2/Neto auxiliary

protein modulates the function of AMPA-subtype ionotropic glutamate receptors. Neuron *75*, 838–850.

Wang, X., Li, G., Liu, J., Liu, J., and Xu, X.Z. (2016). TMC-1 Mediates Alkaline Sensation in C. elegans through Nociceptive Neurons. Neuron *91*, 146–154.

Ward, A., Liu, J., Feng, Z., and Xu, X.Z. (2008). Light-sensitive neurons and channels mediate phototaxis in C. elegans. Nat. Neurosci. *11*, 916–922.

Winter, Z., Gruschwitz, P., Eger, S., Touska, F., and Zimmermann, K. (2017). Cold Temperature Encoding by Cutaneous TRPA1 and TRPM8-Carrying Fibers in the Mouse. Front. Mol. Neurosci. *10*, 209.

Xiao, R., Zhang, B., Dong, Y., Gong, J., Xu, T., Liu, J., and Xu, X.Z.S. (2013). A genetic program promotes C. elegans longevity at cold temperatures via a thermosensitive TRP channel. Cell *152*, 806–817.

STAR★METHODS

KEY RESOURCES TABLE

REAGENT or RESOURCE	SOURCE	IDENTIFIER
Bacterial and Virus Strains		
*E. coli:*OP50	Caenorhabditis Genetics Center	OP50
Chemicals, Peptides, and Recombinant Proteins		
TRIzol LS Reagent	Thermo Fisher Scientific	10-296-010
Power SYBR Green	Thermo Fisher Scientific	4367659
M-MLV Reverse Transcriptase	Thermo Fisher Scientific	28025013
RNAscope 3-plex Negative Control Probe	Advanced Cell Diagnostics	320871
RNAscope 3-plex Positive Control Probe	Advanced Cell Diagnostics	320881
RNAscope Probe Mm-Gluk2	Advanced Cell Diagnostics	438781
L-Glutamic acid	Sigma	49449
Lipofectamine 2000	Thermo Fisher Scientific	11668-019
Fura-2 AM	Thermo Fisher Scientific	F1221
Pluronic F-127	Sigma	P2443
mSIRK	Millipore	371818
YM-254890	WAKO-Chemicals	257-00631
Pertussis Toxin	Thermo Fisher Scientific	PHZ1174
Papain	Sigma	10108014001
Collagenase/Dispase	Sigma	11097113001
4D-Nucleofector™ X Kit	Lonza	V4XP-3024
Critical Commercial Assays		
TruSeq Nano DNA LT Sample Preparation Kit – Set A	Illumina	FC-121-4001
TruSeq Nano DNA LT Sample Preparation Kit – Set B	Illumina	FC-121-4002
Experimental Models: Cell Lines		
CHO	ATCC	CCL-61
COS-7	ATCC	CRL-1651
HeLa	ATCC	CCL-2
Experimental Models: Organisms/Strains		
C. elegans: Strain N2 var. Bristol: wild-type	Caenorhabditis Genetics Center	WB Strain: N2
C. elegans: *glr-3(tm6403)*	Shohei Mitani	WB Strain: *tm6403*
C. elegans: xuIs189[Plfe-2::GCaMP3.0+Plfe-2::DsRed]	This paper	TQ3700
C. elegans: xuIs189[Plfe-2::GCaMP3.0+Plfe-2::DsRed]; glr-3(tm6403)	This paper	TQ5945
C. elegans: xuIs189[Plfe-2::GCaMP3.0+Plfe-2::DsRed]; glr-3(xu261)	This paper	TQ4308
C. elegans: xuIs189[Plfe-2::GCaMP3.0+Plfe-2::DsRed]; xuEx2021[Pges-1::glr-3(gDNA)::SL2::CFP]; glr-3(tm6403)	This paper	TQ5946
C. elegans: xuEx2250[Pges-1::glr-3::SL2::CFP]	This paper	TQ6409
C. elegans: xuEx2021[Pges-1::glr-3(gDNA)::SL2::CFP]; glr-3(tm6403)	This paper	TQ5947
C. elegans: xuEx3000[Pgcy-5::GCaMP6(f)]	This paper	TQ8078
C. elegans: xuEx2902[glr-3(7kb)::sl2::YFP]	This paper	TQ7749
C. elegans: xuEx2994[Pgcy-5::glr-3(cDNA)::sl2::CFP]; glr-3(tm6403)	This paper	TQ8072
C. elegans: xuEX3000[Pgcy-5::GCaMP6(f)]; xuEx2994[Pgcy-5::glr-3(cDNA)::sl2::CFP]; glr-3(tm6403)	This paper	TQ8138
C. elegans: xuEx3144[Pgcy-5::mGluK2::sl2::CFP]; glr-3(tm6403)	This paper	TQ8700
C. elegans: xuEx2383[Pmyo-3::GCaMP6(f)]; xuEx3143[Pmyo-3::mGluk2::sl2::CFP]	This paper	TQ8832

(*Continued on next page*)

Continued

REAGENT or RESOURCE	SOURCE	IDENTIFIER
C. elegans: xuEx3000[Pgcy-5::GCaMP6(f)]; xuEx3144[Pgcy-5::mGluk2::sl2::CFP]; glr-3(tm6403)	This paper	TQ8869
C. elegans: xuEx3000[Pgcy-5::GCaMP6(f)]; unc-31(e169)	This paper	TQ9038
C. elegans: xuEx3000[Pgcy-5::GCaMP6(f)]; unc-13(e51)	This paper	TQ9040
C. elegans: xuEx3000[Pgcy-5::GCaMP6(f)]; eat-4(ky5)	This paper	TQ9045
C. elegans: xuEx2383[Pmyo-3::GCaMP6(f)]; xuEX3175[Pmyo-3::glr-3(cDNA)::sl2::CFP]	This paper	TQ9174
C. elegans: xuEx2383[Pmyo-3::GCaMP6(f)]; xuEx3182[Pmyo-3::glr-3(M582R)::sl2::CFP]	This paper	TQ9175
C. elegans: xuEx2383[Pmyo-3::GCaMP6(f)]; xuEx3184[Pmyo-3::glr-3(Q584R)::sl2::CFP]	This paper	TQ9177
C. elegans: xuEX3000[Pgcy-5::GCaMP6(f)]; xuEx3186[Pgcy-5::glr-3(M582R)::sl2::CFP]; glr-3(tm6403)	This paper	TQ9179
C. elegans: xuEx3000[Pgcy-5::GCaMP6(f)]; xuEx3188[Pgcy-5::glr-3(Q584R)::sl2::CFP]; glr-3(tm6403)	This paper	TQ9180
C. elegans: xuEx2383[Pmyo-3::GCaMP6(f)]; xuEx3191[Pmyo-3::mGluk2(Q622R)::sl2::CFP]	This paper	TQ9228
C. elegans: xuEx2383[Pmyo-3::GCaMP6(f)]; xuEx3197[Pmyo-3::mGluk2(M620R)::sl2::CFP]	This paper	TQ9269
C. elegans: xuEx3000[Pgcy-5::GCaMP6(f)]; xuEx3193[Pgcy-5::mGluk2(Q622R)::sl2::CFP]; glr-3(tm6403)	This paper	TQ9227
C. elegans: xuEx3000[Pgcy-5::GCaMP6(f)]; xuEx3200[Pgcy-5::mGluk2(M620R)::sl2::CFP]; glr-3(tm6403)	This paper	TQ9271
C. elegans: xuEx3000[Pgcy-5::GCaMP6(f)]; gpa-3(pk35)	This paper	TQ9289
C. elegans: xuEx3000[Pgcy-5::GCaMP6(f)]; goa-1(n1134)	This paper	TQ9290
C. elegans: xuEx3000[Pgcy-5::GCaMP6(f)]; gpa-3(pk35); goa-1(n1134)	This paper	TQ9291
C. elegans: xuEx3000[Pgcy-5::GCaMP6(f)]; che-2(e1033)	This paper	TQ9667
C. elegans: xuEx3251[Pgcy-5::goa-1(cDNA)::sl2::mcherry2]; xuEx3000[Pgcy-5::GCaMP6(f)]; goa-1(n1134)	This paper	TQ9625
C. elegans: xuIs259 [Plfe-2::GCamp3.0+Plfe-2::DsRed]; goa-1(n1134)	This paper	TQ9671
C. elegans: xuIs259 [Plfe-2::GCamp3.0+Plfe-2::DsRed]; glr-3(xu261)	This paper	TQ9741
C. elegans: xuIs259 [Plfe-2::GCamp3.0+Plfe-2::DsRed]; trpa-1(ok999); glr-3(tm6403)	This paper	TQ9740
Oligonucleotides		
siRNA targeting sequence: GluK2 #1:ACGCAGATTGGTGGCCTTATA	This paper	N/A
siRNA targeting sequence: GluK2 #2:AAGGTACAATCTTCGACTTAA	This paper	N/A
siRNA targeting sequence: GluK2 #3:TCGCTTCATGAGCCTAATTAA	This paper	N/A
siRNA targeting sequence: GluK2 #4:TACAGGCAGAATTACATTTAA	This paper	N/A
Primer: For qPCR mGluK2: fwd: GCGCAACCATGACGTTTTTCAAG	This paper	N/A
Primer: For qPCR mGluK2: rev: CCATGGGAGTGCCAACACCATAG	This paper	N/A
Primer: For glr-3 promoter: fwd: TTAATTCACATTCCATCGGAAAAATC	This paper	N/A
Primer: For glr-3 promoter: rev: GCCTAGTGACTCGGTCTCTACTCGTA	This paper	N/A
Recombinant DNA		
Plasmid: Pglr-3::sl2::YFP	This paper	pSX2074
Plasmid: Pgcy-5::glr-3(cDNA):sl2::CFP	This paper	pSX2101
Plasmid: Pmyo-3::glr-3(cDNA)::sl2::mcherry	This paper	pSX2120
Plasmid: PcDNA3.1-Flag-glr-3(cDNA)	This paper	pSX2177
Plasmid: PcDNA3.1+N-DYK-hGluK2	GenScript	OHu23233
Plasmid: PcDNA3.1+N-DYK -mGluK2	GenScript	OMu13059
Plasmid: PcDNA3.1+N-DYK -fGluK2	GenScript	ODa42289
Plasmid: Pmyo-3::mGluK2::sl2::CFP	This paper	pSX2191
Plasmid: Pgcy-5::mGluK2::sl2::CFP	This paper	pSX2192
Plasmid: PcDNA3.1-Flag-glr-3(cDNA,M582R)	This paper	pSX2791

(*Continued on next page*)

Continued

REAGENT or RESOURCE	SOURCE	IDENTIFIER
Plasmid: PcDNA3.1-Flag-glr-3(cDNA,Q584R)	This paper	pSX2792
Plasmid: PcDNA3.1-Flag-glr-3(cDNA,P121L)	This paper	pSX2869
Plasmid: PcDNA3.1-Flag-glr-3(cDNA,P130L)	This paper	pSX2870
Plasmid: Pmyo-3::glr-3(cDNA,M582R)::sl2::mcherry	This paper	pSX2795
Plasmid: Pmyo-3::glr-3(cDNA,Q584R)::sl2::mcherry	This paper	pSX2796
Plasmid: Pgcy-5::glr-3(cDNA,M582R):sl2::CFP	This paper	pSX2793
Plasmid: Pgcy-5::glr-3(cDNA,Q584R):sl2::CFP	This paper	pSX2794
Plasmid: PcDNA3.1-Flag-mGluK2(M620R)	This paper	pSX2797
Plasmid: PcDNA3.1-Flag-mGluK2(Q622R)	This paper	pSX2798
Plasmid: PcDNA3.1-Flag-mGluK2(P151L)	This paper	pSX2868
Plasmid: Pmyo-3::mGluK2(M620R)::sl2::CFP	This paper	pSX2802
Plasmid: Pmyo-3::mGluK2(Q622R)::sl2::CFP	This paper	pSX2803
Plasmid: Pgcy-5::mGluK2(M620R)::sl2::CFP	This paper	pSX2800
Plasmid: Pgcy-5::mGluK2(Q622R)::sl2::CFP	This paper	pSX2801
Plasmid: Pgcy-5::goa-1(cDNA)::sl2::CFP	This paper	pSX2822
Software and Algorithms		
MetaFluor	Molecular Devices Inc.	N/A
GraphPad	GraphPad Software, Inc	N/A

LEAD CONTACT AND MATERIALS AVAILABILITY

Further information and requests for resources and reagents should be directed to and will be fulfilled by the Lead Contact, X.Z. Shawn Xu (shawnxu@umich.edu). This study has generated plasmids and *C. elegans* strains, which are listed in the Key Resources Table. These reagents will be made available upon request.

EXPERIMENTAL MODEL AND SUBJECT DETAILS

C. elegans strains were maintained at 20°C on nematode growth medium (NGM) plates seeded with OP50 bacteria unless otherwise specified. Transgenic lines were generated by injecting plasmid DNA directly into hermaphrodite gonad. Mutant strains and integrated transgenic strains were outcrossed at least six times before use.

CHO cells were cultured in DMEM/F12 media with 10% FBS (heat-inactivated) at 37°C under 5% CO2. DMEM media with 10% FBS (heat-inactivated) were used to culture COS-7 and HeLa cells. These cell lines were obtained from the ATCC. See Key Resources Table for details.

METHOD DETAILS

Molecular biology and genetics

For the experiments involving transgenes, two to three independent transgenic lines were tested to confirm the results. *glr-3* cDNA was cloned by RT-PCR from total RNA isolated from WT (N2) worms. The expression of the transgene was verified by CFP, YFP or mCherry expression, which was driven by SL2 from the same transcript. Mouse, human and zebrafish GluK2 cDNA plasmids were obtained from GenScript (all in the pcDNA3.1+N-DYK vector). See Key Resources Table for plasmid information.

Genetic screen

EMS was used to mutagenize worms carrying a transgene co-expressing GCaMP and DsRed, which enables ratiometric detection of changes in GCaMP fluorescence by a real-time qPCR thermocycler (ABI 7500). Worms from each F2 plate were washed with M9 buffer and transferred to an unseeded NGM plate to clean off bacteria. Five individual worms from each strain were picked to a well of a 96-well plate with 20 μL recording buffer (10 mM HEPES at pH 7.4, 5 mM KCl, 145 mM NaCl, 1.2 mM MgCl2, 2.5 mM CaCl2, 10 mM glucose). PCR plates were loaded onto a real-time qPCR thermocycler and cooled from 23°C to 10°C. Those candidates that failed to respond to cooling were recovered and outcrossed to the parental strain for six times. Both the parental and mutant strains were then subjected to whole-genome sequencing (WGS). Analysis of the sequencing data was done as described (Minevich et al., 2012). By comparing the WGS data between parental and mutant strain, we obtained a density map of single nucle-

otide variants and mapped the mutation in *xu261* to the gene *glr-3*, which mutated P121 residue to L. By testing the deletion null mutant *glr-3(tm6403)*, we found that it exhibited the same cold-sensing phenotype as *glr-3(xu261)* in the intestine, which was rescued by transgenic expression of wild-type *glr-3* gene in the intestine.

C. elegans calcium imaging and behavioral assays

Calcium imaging was performed on an Olympus IX73 inverted microscope under a 40X objective. Images were acquired using an ORCA-Flash 4.0 sCMOS camera (Hammatsu Inc.) with MetaFluor software (Molecular Devices Inc.). To image the intestine, ASER neuron and body-wall muscle cells in response to temperature stimuli, we glued worms on a cover glass covered with a thin layer of agarose pad. A Bipolar In-line Cooler/Heater (SC-20 from Warner Instruments) was used to control the temperature of the recording solution, which was perfused toward the worm. Recording buffer: 10 mM HEPES at pH 7.4, 5 mM KCl, 145 mM NaCl, 1.2 mM MgCl2, 2.5 mM CaCl2, 10 mM glucose. The temperature was initially set at 23°C; after achieving a basal line, the temperature was cooled to 10°C over 120 s, and heated back to 23°C. Faster cooling can be achieved by perfusing pre-cooled (4°C) solution toward the subject, and similar results were obtained (Figures S2A–S2F); but since this protocol does not permit precise control of the end temperature, we focused on the use of the former. To image ASER neuron in response to salt gradient, we used a microfluidic system as described previously (Wang et al., 2016). Briefly, worms were loaded into the chip mounted on the microscope, and 50 to 0 mM salt concentration steps were performed by switching solutions administered to the nose tip (25 mM potassium phosphate [pH 6.0], 1 mM $CaCl_2$, 1 mM $MgSO_4$, 0.02% gelatin, and either 50 or 0 mM NaCl with glycerol to adjust osmolarity to 350 mOsm). For intestine calcium imaging, we scored the peak percentage change in the ratio of GCaMP/DsRed fluorescence. For ASER and muscle imaging, we scored the peak percentage change in in the intensity of GCaMP fluorescence.

Cooling-evoked swimming assay was performed in a recording chamber (RC-26 from Warner Instruments) filled with M9 buffer using day 1 adult hermaphrodites. The temperature was initially set at 21°C, gradually cooled to 18°C over 40 s, and then heated back to 21°C by slowly perfusing the chamber with M9 buffer of varying temperatures with a Bipolar In-line Cooler/Heater (Warner Instruments). The number of turns that worms displayed every 10 s was scored.

Cooling-evoked probe assay was performed in an environmentally controlled room set at 21°C and 30% humidity. Day 1 adult hermaphrodites were tested. Animals were tested on standard NGM plates dried for one hour without lids to remove any excess surface moisture. Prior to testing, plates were seeded with a thin lawn of fresh OP50 in the center of the plate to prevent animals from leaving, which was allowed to dry for 10 minutes prior to placing animals on the plate. To deliver localized cooling stimuli to a region of the worm, we used a custom-built thermoelectric cooling probe with a tip size of 50 μm. The design and fabrication of the cooling device will be described elsewhere. The probe tip was pre-cooled to 17°C and placed ~100 μm above the head of the animal (without touching the animal) for 5 s using a micromanipulator. An avoidance response was scored if the worm stopped forward movement and initiated a reversal with at least half a head swing within the 5 s period. Five animals were tested on a single plate. Each animal was tested only once as we observed *C. elegans* could quickly adapt to acute cooling stimuli, resulting in a blunted response upon multiple trials. The response rate for five animals on one plate was averaged and counted as a single trial, and repeated for a total of 10 trials per genotype.

Salt chemotaxis assay was carried out as previously described (Tomioka et al., 2006). Briefly, young adult animals were collected, washed, and transferred with chemotaxis buffer (25 mM potassium phosphate (pH 6.0), 1 mM $CaCl_2$, 1 mM $MgSO_4$) followed by a final wash in ddH_2O. Test plates were made using 10 cm diameter assay plates (5 mM KPO_4, pH 6.0, 1 mM $CaCl_2$, 1mM $MgSO_4$, 2% agar), on which a salt gradient was formed by placing a 2% agar plug (10 mm diameter) made in chemotaxis buffer containing 100 mM of NaCl. Fifty to two hundred animals were tested for each plate. The chemotaxis index (C.I.) was calculated as described previously (Tomioka et al., 2006).

Cell culture and calcium imaging

CHO cells were cultured in DMEM/F12 media with 10% FBS (heat-inactivated) at 37°C under 5% CO2. DMEM media with 10% FBS (heat-inactivated) were used to culture COS-7 and HeLa cells. Cells grown on cover glasses coated with poly-lysine were transfected in 35 mm dishes using Lipofectamine 2000 (ThermoFisher) for 4 hours. The lipid/DNA ratio was 3:1, and the total DNA was 1.5 μg except for fish GluK2. For fish GluK2, to maximize its expression level, we used 12 μL lipid and 3 μg DNA for transfection.

18 hours after the transfection, cells were loaded with 4 μM Fura-2 AM and 0.2% Pluronic F127 in HBSS buffer at 37°C for 30 min, washed for 3 times with HBSS, and incubated in the recording buffer for 30 min before calcium imaging. It is important to use a ratiometric dye such as Fura-2 to image cold responses, as single wavelength dyes may show intrinsic responses to cold. Recording buffer: 10 mM HEPES at pH 7.4, 5 mM KCl, 145 mM NaCl, 1.2 mM MgCl2, 2.5 mM CaCl2, 10 mM glucose. Calcium imaging was performed as described above for *C. elegans* imaging with the following modification: to obtain better Fura-2 images under 340/380 nm, we used a 40x water-immersion objective with high transmission efficiency of UV light. The same temperature control protocol was used as described above for *C. elegans* imaging. For those experiments involving inhibitors, cells were pretreated with inhibitors (mSIRK: 50 μM; YM-254890: 10 μM) right after Fura-2 AM loading. For PTX, we pretreated cells with 100 ng/ml of PTX for 10 hours before the imaging experiment.

Mouse DRG neuron culture, transfection, qPCR, and calcium imaging

DRG culture and siRNA transfection were carried out as described previously (Lou et al., 2013). Briefly, mice were euthanized at the age of P14-15 by CO2 inhalation using a protocol approved by the Institutional Animal Care and Use Committee at University of Michigan. DRGs were isolated from T10-L6 and collected in Ca^{2+}- and Mg^{2+}-free Hank's buffered salt solution (HBSS). Following isolation, DRGs were digested with papain (1.5 mg/ml, MilliporeSigma) for 10 minutes and then collagenase/dispase for 12 minutes (1 mg/ml, MilliporeSigma) at 37°C. After digestion, the culture was then triturated and dissociated using fire-polished Pasteur pipettes for further siRNA transfection. To knockdown GluK2 mRNA transcripts, a pool of 4 different siRNA (250 nM, QIAGEN. Target sequences: ACGCAGATTGGTGGCCTTATA, AAGGTACAATCTTCGACTTAA, TCGCTTCATGAGCCTAATTAA, TACAGGCAGAATTACATTTAA) was electroporated into the freshly dissociated DRG neurons using P3 Primary Cell 4D-Nucleofector™ X Kit (V4XP-3024, Lonza). A scrambled siRNA (250 nM, QIAGEN) was transfected as a control. A MaxGFP construct (1 μl, Lonza) was co-transfected as a marker.

Two days post-transfection, DRG neurons were harvested, and the total RNA was extracted with TRIzol (Life Technologies) for quantitative real-time PCR (qPCR) analysis. qPCR reactions were performed in a 384-well format using Power SYBR Green (Thermo Fisher Scientific). Relative mRNA levels were calculated using the $\Delta\Delta C_T$ method and normalized to *Tbp, 36B4*. Primer sequences: mGluK2 fwd: GCGCAACCATGACGTTTTTCAAG, mGluK2 rev: CCATGGGAGTGCCAACACCATAG.

Calcium imaging of cultured DRG neurons was carried out two days post-transfection. The imaging protocol was similar to that described above for CHO cell imaging, except that a 20x rather than 40x water-immersion objective with high transmission efficiency of UV light was used for imaging. DRG neurons showing $\geq$ 25% increase in fura-2 F_{340}/F_{380} fluorescence ratio ($\Delta R/R$) in response to temperature stimulation were scored positive.

Mouse DRG *in situ* hybridization (RNAscope)

PFA-fixed DRG samples from P30 mice was frozen in optimal cutting temperature (OCT) freezing medium and then the DRGs were used to prepare six adjacent sections at 12 μm thickness. GluK2 mRNA transcript in the DRG sections was detected using RNAscope assay (Wang et al., 2012a). The probes were designed and provided by Advanced Cell Diagnostics, Inc (Advanced Cell Diagnostics, Newark, CA). Staining was performed using the RNAscope multiplexed fluorescent *in situ* hybridization kit, according to manufacturer's instructions. For quantification of GluK2-positive population, neurons that had at least four positive signals (observed as puncta) within the periphery of the neurons, as defined by the phase contrast image, were considered as GluK2-positive. Around 300-450 neurons from each animal were analyzed for GluK2 mRNA transcripts. For categorization of GluK2-positive neuronal population, the type of the neurons was assigned by measuring their size. Only the neurons containing nuclei were counted. As described previously (Fang et al., 2005), neurons with a surface area < 400 μm^2, 400-800 μm^2, and > 800 μm^2 were categorized as small-diameter, medium-diameter and large-diameter cells, respectively.

Electrophysiology

Whole-cell patch-clamp recording was performed on an Olympus IX73 inverted microscope under a 40x objective with a Multiclamp 700B amplifier. Transfected cells were identified with a co-transfection RFP marker. Bath solution (in mM): 145 NaCl, 2.5 KCl, 1 $CaCl_2$, 1 $MgCl_2$, 10 glucose, and 5 HEPES (pH adjusted to 7.2). Pipette solution: 115 K-gluconate, 15 KCl, 1 $MgCl_2$, 10 HEPES, 0.25 $CaCl_2$, 20 sucrose, 5 BAPTA, and 5 Na_2ATP. Glutamate (10 mM) was diluted in bath solution and perfused toward the cell using a rapid perfusion system (Bio-Logic) to evoke glutamate-gated currents. Pipette resistance: 2-4 MΩ. Series resistance and capacitance were compensated during recording. Voltage was clamped at −70 mV.

QUANTIFICATION AND STATISTICAL ANALYSIS

Quantification and statistical parameters were indicated in the legends of each figure, including the statistical method, error bars (SEM), n numbers, and p values. We applied ANOVA, t test, and χ^2 test to determine statistical significance. Specifically, for those analyses involving multiple group comparisons, we applied one-way ANOVA followed by a post hoc test (Bonferroni test). For those only involving two groups, we applied t test (Figure 7C) and χ^2 test (Figure 7F). We considered p values of < 0.05 significant. All analyses were performed using SPSS Statistics software (IBM, Inc).

DATA AND CODE AVAILABILITY

This study did not generate/analyze datasets or code.

Cell

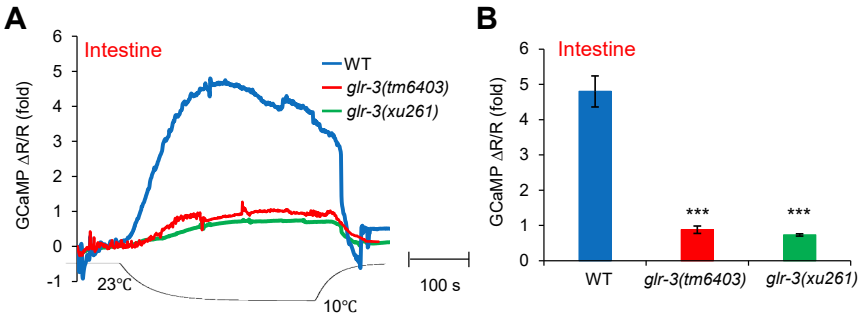

Figure S1. Additional Data Regarding Cooling-Evoked Calcium Response in the Intestine, Related to Figure 1

(A and B) Both *glr-3(tm6403)* and *glr-3(xu261)* mutant worms showed a severe defect in cooling-evoked calcium response in the intestine. (A) Sample traces. (B) Bar graph. Error bars: SEM n $\geq$ 10. ***p < 0.0001 (ANOVA with Bonferroni test).

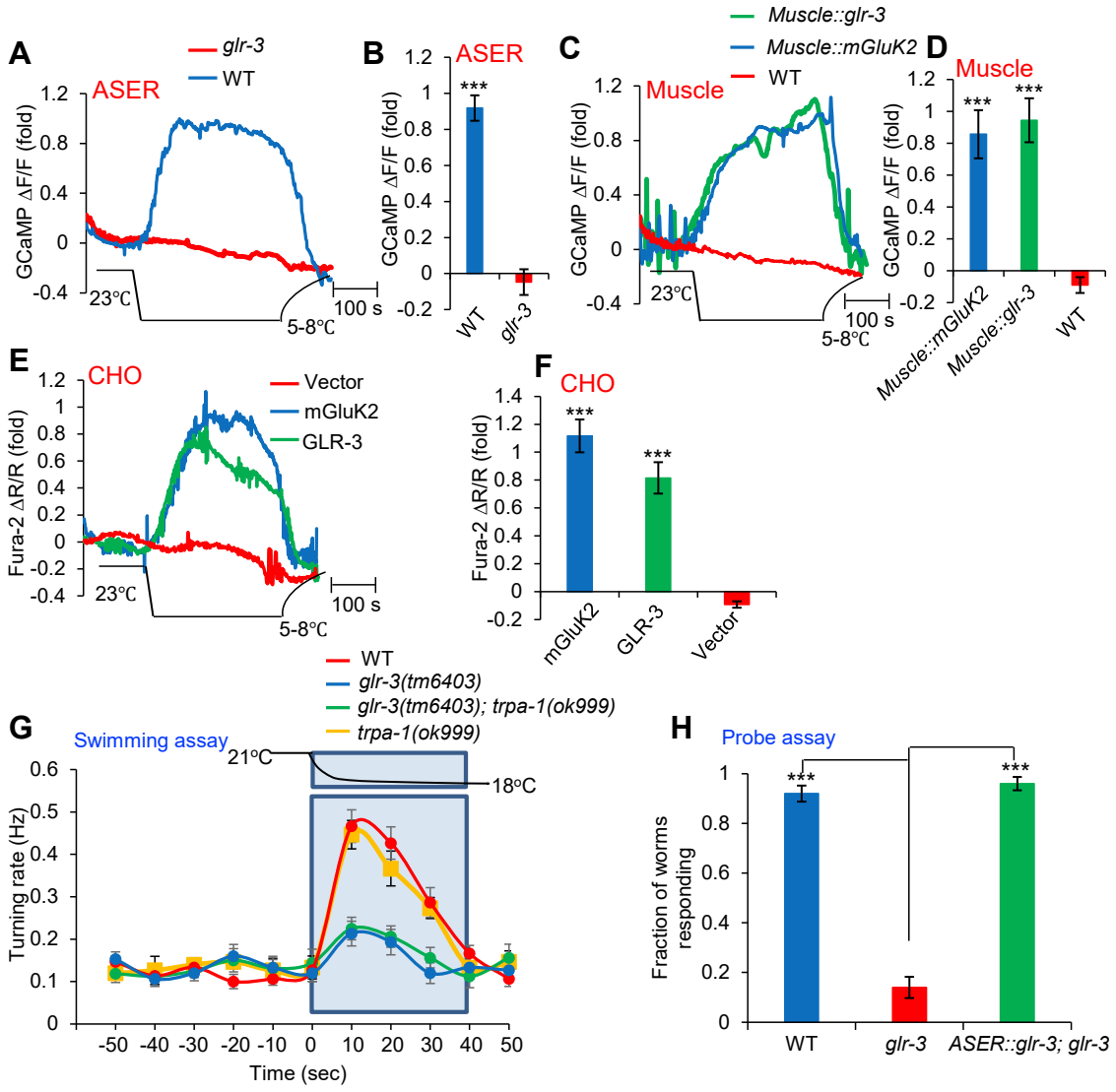

Figure S2. Rapid Cooling Evokes GLR-3/GluK2-Dependent Calcium Response in *C. elegans* (ASER Neuron and Muscles) and CHO Cells and Additional Data on Cold-Avoidance Behavior, Related to Figures 2 and 3

(A–F) Rapid cooling was achieved by perfusing pre-cooled solution toward the worm or CHO cells that express GLR-3/GluK2. We observed cooling-evoked calcium response similar to that described in the main figures. But since this protocol did not permit precise control of the end temperature from experiment to experiment (varying from 5-8°C), we focused on the use of the conventional cooling protocol. Error bars: SEM n ≥ 12. ***p < 0.0001 (ANOVA with Bonferroni test).

(G) TRPA-1 is not involved in cold-avoidance behavior in a swimming assay.

(H) *glr-3(tm6403)* mutant worms are defective in cold-avoidance behavior in a probe assay, which was rescued by an ASER-specific *glr-3* transgene. A pre-cooled probe, which cooled the air temperature near the head of the worm crawling on an agar plate, triggered backward movement (reversals). Error bars: SEM n ≥ 10. ***p < 0.0001 (ANOVA with Bonferroni test).

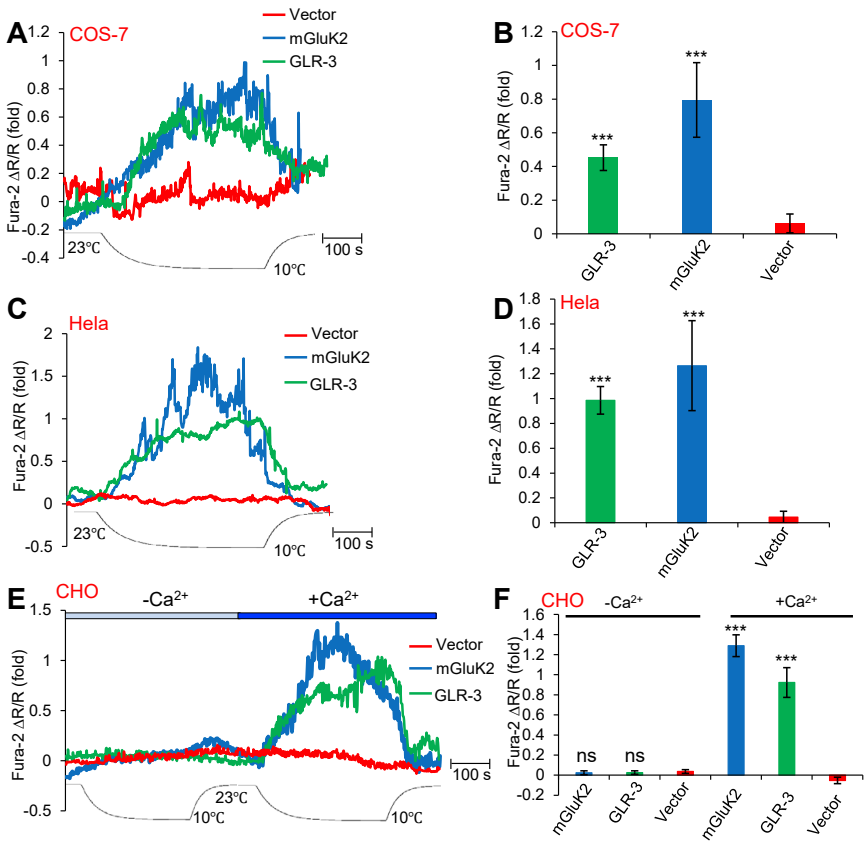

Figure S3. Heterologous Expression of GLR-3 and Mouse GluK2 in COS-7 and HeLa Cells Confers Cold Sensitivity, and Cooling-Evoked Calcium Increase Mediated by GLR-3/GluK2 Primarily Results from Calcium Influx, Related to Figure 3

(A–D) COS-7 cells and HeLa cells were transfected with GLR-3 and mGluK2 or vector control. Cooling evoked calcium response in GLR-3 and mGluK2 transfected cells but not control cells. (A-B) COS-7 cells. Error bars: SEM $n \geq 15$. ***$p < 0.0001$ (ANOVA with Bonferroni test). (C-D) HeLa cells. Error bars: SEM $n \geq 20$. ***$p < 0.0001$ (ANOVA with Bonferroni test).

(E and F) Cooling-evoked calcium increase mediated by GLR-3/GluK2 primarily results from calcium influx. Cooling evoked no or little calcium response in GLR-3/GluK2-expressing CHO cells in the absence of extracellular calcium, but evoked robust calcium increase when calcium was present in the bath solution. (E) Sample traces. (F) Bar graph. Error bars: SEM $n \geq 18$. $p = 0.601$, $p = 0.773$, ***$p < 0.0001$ (ANOVA with Bonferroni test).

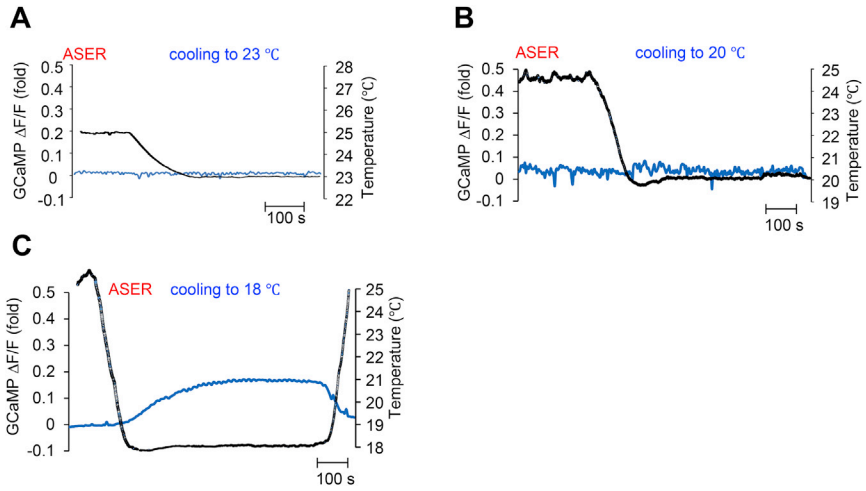

Figure S4. Cooling to 18°C Evokes Calcium Response in ASER Neuron, Related to Figure 4

(A–C) Sample traces showing that the activation threshold of ASER neuron is around 18°C. Cooling to 23°C (A) and 20°C (B) failed to evoke calcium response in ASER neuron, while cooling to 18°C did (C). The traces in blue represent calcium traces, while those in black denote temperature changes.

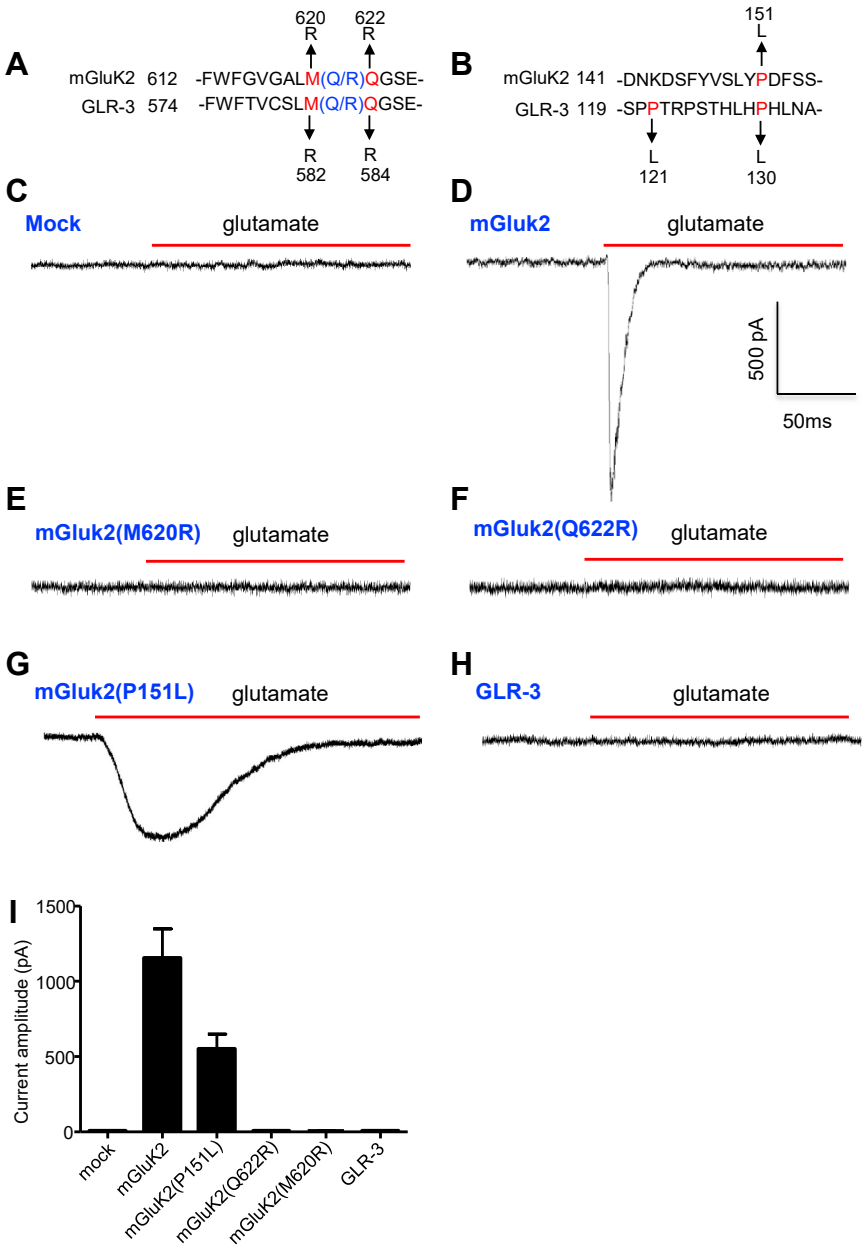

Figure S5. Glutamate-Gated Current Is Only Detected in Mouse GluK2 but Not the Channel-Dead Mouse GluK2 Variants or GLR-3, Related to Figures 4 and 5

(A) Sequence alignment of mouse GluK2 and GLR-3 in the M2 pore region. The Q/R RNA editing site is denoted in blue. The residues mutated in this study are marked in red.

(B) Sequence alignment mouse GluK2 and GLR-3 in the N-terminal ATD domain where point mutations were generated in this study. The residues mutated are marked in red.

(C–I) Whole-cell recording of glutamate-gated currents of wild-type and various variants of mouse GluK2 as well as GLR-3 expressed in CHO cells. Glutamate: 10 mM. (C-H) Sample traces. (I) Bar graph. n $\geq$ 4. Error bars: SEM.

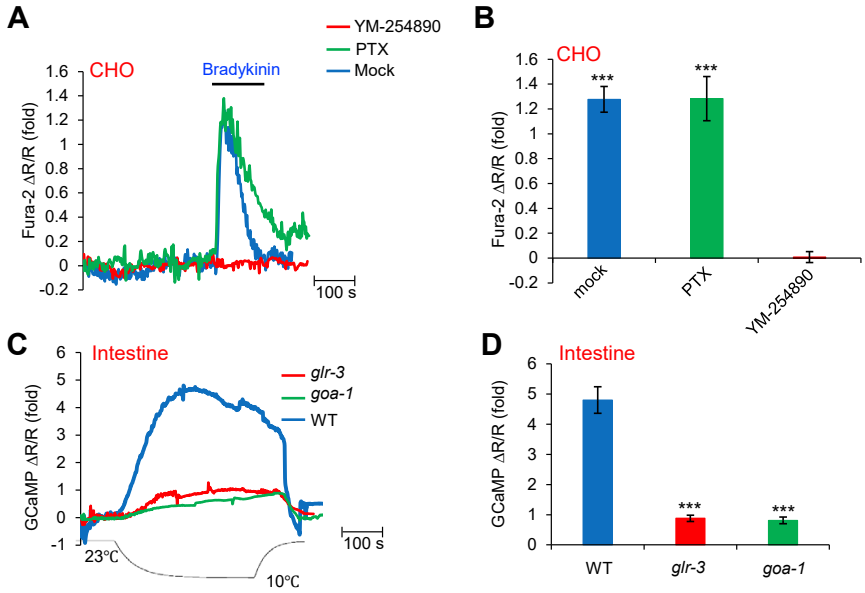

Figure S6. Additional Data on G Protein Signaling in CHO Cells and Cooling-Evoked Calcium Response in *C. elegans* Intestine, Related to Figure 6

(A and B) Bradykinin-evoked calcium response in CHO cells is sensitive to the Gq/11 inhibitor YM-254890 but not the Gi/o inhibitor PTX. Bradykinin (10 μM) evoked robust calcium response in CHO cells, which was blocked by pre-incubation with YM-254890 (10 μM) but not by PTX (100 ng/ml). (A) Sample traces. (B) Bar graph. Error bars: SEM $n \geq 20$. ***$p < 0.0001$ (ANOVA with Bonferroni test).

(C andD) *goa-1(n1134)* and *glr-3(tm6403)* mutant worms show a severe defect in cooling-evoked calcium response in the intestine. (C) Sample traces. (D) Bar graph. Error bars: SEM $n \geq 10$. ***$p < 0.0001$ (ANOVA with Bonferroni test). The WT and *glr-3(tm6403)* sample traces and data are identical to those in Figure S1 and are included for the purpose of comparison. These experiments were carried out along with *glr-3(xu261)* mutant worms shown in Figure S1 at the same time.